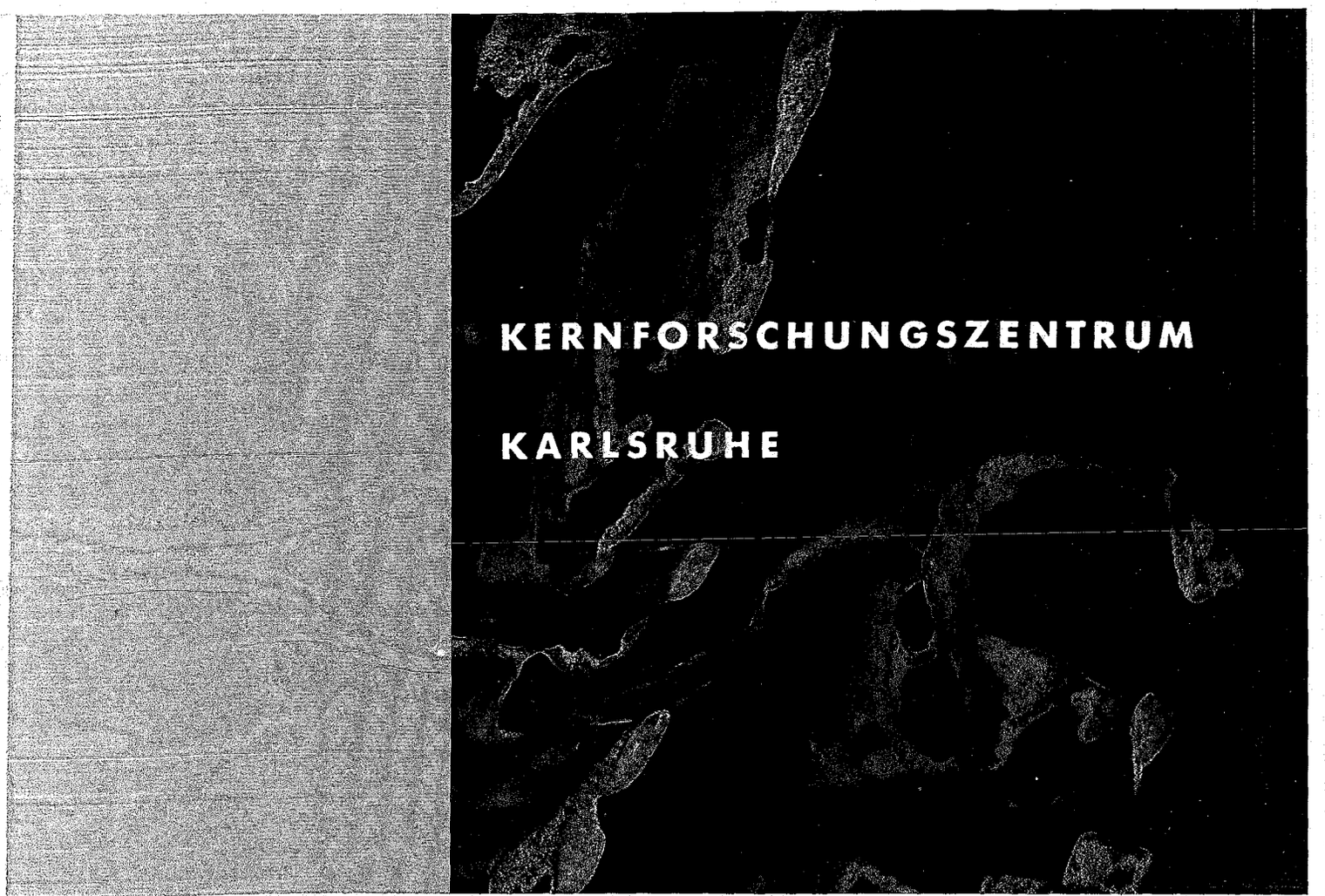

März 1971 KFK 1384

Institut für Material- und Festkörperforschung
Projekt Schneller Brüter

Room temperature mechanical properties and precipitation behaviour of Steel X8CrNiMoVNb 1613 (4988), Incoloy 800 and Inconel 718 after annealing in contact with UC at 600°C to 800°C.

W. E. Stumpf, O. Götzmann

GESELLSCHAFT FÜR KERNFORSCHUNG M. B. H.
KARLSRUHE

GESELLSCHAFT FÜR KERNFORSCHUNG M.B.H.
KARLSRUHE

KERNFORSCHUNGSZENTRUM KARLSRUHE

März 1971 KFK 1384

Institut für Material- und Festkörperforschung

Projekt Schneller Brüter

Room temperature mechanical properties and precipitation behaviour of Steel X8CrNiMoVNb 1613 (4988), Incoloy 8oo and Inconel 718 after annealing in contact with UC at 6oo°C to 8oo°C.

von

W.E. Stumpf *)

O. Götzmann

GESELLSCHAFT FÜR KERNFORSCHUNG mbH., KARLSRUHE

---

*) Delegate from the Atomic Energy Board, Pretoria, South Africa

---

3o.3.71

Abstract

The room temperature mechanical properties and the precipitation behaviour was studied in tensile test specimens that had been annealed in UC powder (4.84 % equivalent C) and in vacuum respectively, for times up to 1100 hours at 600, 700 and 800°C. An electron microscope technique was developed which made the examination of the reaction products in the alloys, at the reaction interface, possible.

Steel 4988 showed a considerable decrease in mechanical strength, after annealing in UC, at all three temperatures. For example, after 1100 hours at 700°C in contact with the UC the 0.2 % yield strength had dropped by 30 %. No carburisation of the specimens was found, however, and the ductility remained unaffected. This behaviour is caused by the partial dissolution of the NbC and V(CN) precipitates in the steel near the reaction interface.

The room temperature strength properties of Incoloy 800 in the millannealed condition, after annealing in UC at 600°C, are decreased but the ductility is unaffected. At 700 and 800°C, in both the millannealed and in the solution treated condition, however, the strength properties are unaffected but the ductility is reduced by the UC. For both initial conditions, extensive precipitation of $M_{23}C_6$ is found near the reaction interface and in the solution treated condition enhanced precipitation of TiC also occurs after annealing in UC.

Inconel 718 was affected in a complex way by the UC. After annealing in UC at 600°C no effect was found on the strength properties but the ductility was decreased to only a few percent elongation after 1100 hours. After annealing at 700°C the strength and ductility are decreased by the UC and at 800°C practically no effect on the yield strength, a decrease in tensile strength and a very small increase in ductility was found. At all three temperatures a M_6C phase is formed in the alloy at the reaction interface while, at the same time, the niobium-containing precipitates $Ni_3(NbAlTi)$ and Ni_3Nb are dissolved, causing the observed effects on the mechanical properties.

Kurzfassung

Die mechanischen Eigenschaften und das Ausscheidungsverhalten bei Raumtemperatur wurden an Flachzerreißproben untersucht, die in UC Pulver (4,84 % Äquivalent C) und im Vakuum bei 600, 700 und 800°C bis zu 1100 Stunden geglüht wurden. Es wurde eine Methode entwickelt, die es ermöglichte, mit dem Elektronenmikroskop die Reaktionsprodukte in den Legierungen an der Reaktionsgrenzfläche zu untersuchen.

Der Stahl vom Typ 4988 erfuhr eine beträchtliche Abnahme der Festigkeit bei allen drei Temperaturen. So fiel z.B. nach 1100 Stunden bei 700°C im Kontakt mit UC die 0,2 % Fließgrenze um 30 % ab. Es wurde jedoch keine Aufkohlung der Proben festgestellt, auch wurde die Duktilität nicht beeinflußt. Dieses Verhalten wird durch die teilweise Auflösung der NbC und V(CN) Ausscheidungen im Stahl nahe der Reaktionsgrenzfläche verursacht.

Die Raumtemperatur-Festigkeitseigenschaften von Incoloy 800 im Anlieferungszustand werden nach einer Glühung in UC bei 600°C vermindert; die Duktilität wird aber nicht beeinflußt. Durch die Glühung in UC bei 700 und 800°C jedoch werden sowohl im Anlieferungszustand wie im lösungsgeglühten Zustand die Festigkeitseigenschaften nicht verändert, die Duktilität aber vermindert. Bei beiden Ausgangszuständen wird eine ausgeprägte Ausscheidung von $M_{23}C_6$ nahe der Reaktionsgrenzfläche gefunden und beim lösungsgeglühten Zustand findet eine verstärkte Ausscheidung von TiC nach der Glühung in UC statt.

Inconel 718 wurde auf vielfältige Weise durch das UC beeinflußt. Nach Glühung in UC bei 600°C wurde keine Wirkung auf die Festigkeitseigenschaften gefunden; die Duktilität wurde aber nach 1100 Stunden bis auf wenige Prozent Dehnung herabgesetzt. Nach 700°C in UC wird die Festigkeit und Duktilität vermindert, und nach 800°C wurde praktisch keine Wirkung auf die Fließgrenze, aber eine Abnahme der Bruchfestigkeit und eine geringe Erhöhung der Duktilität gefunden. Bei allen drei Temperaturen wird eine M_6C Phase in der Legierung bei der Reaktionsgrenzfläche gebildet, während zur gleichen Zeit die niobhaltigen Ausscheidungen Ni_3(NbAlTi) und Ni_3Nb aufgelöst werden, was die beobachteten Wirkungen auf die mechanischen Eigenschaften verursacht.

1. Introduction

One of the deciding factors in the selection of a cladding material for a nuclear reactor is the resistance to undesirable interactions with the fuel which can lead to a premature cladding rupture. In the sodium-cooled fast reactor fuelled with a carbide fuel, this problem assumes great importance because of the high temperatures involved and the relatively strong carburising potential of UC and some of its higher carbides. The effects of incompatibility interactions with UC on the room temperature tensile properties has, therefore, been studied at temperatures between 600 and 800°C on the steel 4988, Incoloy 800 and Inconel 718. The latter two alloys are not very strong candidates for application in a reactor of the above type but were included in this investigation for comparison purposes to the more ideally suited steel 4988.

Very little has been published on the mechanical properties of cladding materials as affected by incompatibility with UC, although some bend tests after annealing in contact with UC have given some indication of the carbon uptake that can be tolerated before gross embrittlement sets in [1, 2]. Substantially more work has been done on the changes in mechanical properties of cladding materials after treatment in carbon-contaminated sodium [3, 4]. In general it was found that in most stainless steels the yield and tensile strengths remained unaffected but that the ductility was reduced by the carbon uptake, reductions of up to $\frac{1}{2}$ in the elongation being reported [3].

In this work an electron microscope technique made it possible to pay close attention to the structures, morphologies and sites of nucleation of the reaction products appearing in the cladding materials and in most of the cases these observations could be satisfactorily correlated with the changes in mechanical properties after annealing in contact with UC. In a preliminary investigation [5] the annealing behaviour of these alloys at the same temperatures but in vacuum, had been correlated with the room temperature tensile properties. In this report these results are used as a base-line so that effects caused by the annealing treatment in UC can be seperated from the changes in mechanical properties caused by the normal precipitation behaviour.

2. Experimental procedure

The alloys were received in sheet-form with nominal thickness 1 mm and from these, tensile test specimens with a gauge length of 22 mm, as shown in fig. 1, were die-pressed. The composition of each steel is given in Table I.

These tensile test specimens were then given the following initial heat treatments: steel 4988 was solution treated and then age-hardened for 3 hours at 750°C; one batch of Incoloy 800 was annealed and another was solution treated and finally the Inconel 718 was solution treated. The exact heat treatments and resulting grain sizes are given in Table II. The specimens were then given a light electropolish to remove any oxide film [5].

The uranium carbide was received in the form of cast bars from the firm NUKEM as melt no. 14 and these bars were then crushed and ground to a size fraction 25 to 63 microns. All these operations were carried out under doubly distilled decahydronaphtaline ($C_{10}H_{18}$) to prevent oxidation of the UC powder. The composition of this powdered UC is given in Table III. Due to a slight oxygen and nitrogen pickup the UC was very slightly overstoichiometric although no second phase could be identified upon microstructural examination. This UC powder (still under "decalin") was then vibrated into the steel capsules containing the specimens (see fig. 1) until the entire specimens were covered. The capsules were then placed in silica tubes and evacuated to 10^{-4} mm Hg before being finally sealed off. Because of the "decalin" still in the UC this evacuation took up to 24 hours but could be speeded up by placing a boiling water bath around the silica capsules. The final density of the dry UC powder was only 65 % of the theoretical density. These capsules were then annealed in muffle furnaces at 600, 700 and 800°C for times of 100, 300, 700 and 1100 hours. The Incoloy 800 in the solution treated condition was annealed at 700 and 800°C only.

After completion of the annealing treatments in UC the room temperature tensile properties were determined at a tensile strain rate of 1.3×10^{-3}/sec. The 0.2 % yield strength, the ultimate tensile strength and the elongation were determined from two seperate specimens for each final heat treatment and the average value of the two used in the final evaluation. These tensile mechanical properties could then be compared to those

obtained after annealing in vacuum without UC [5]. One half of the tensile test specimen was then electroplated with nickel prior to the preparation of a carbon extraction replica from a section of the specimen, as has been described elsewhere [5, 6]. The purpose of the nickel plating was to ensure that the extraction replica could be examined right up to the edge of the specimen which had been in contact with the UC, as described in Appendix I. Apart from electron diffraction analysis of any new phases in the alloys, some volume fraction determinations of the NbC phase in steel 4988 were made near the edge of the specimens which had been in contact with the UC and were then compared to the volume fractions in the center of the specimens i.e. the normal volume fractions. For this purpose about looo particles were measured by a Zeiss particle analyser for each determination and the volume fraction calculated as described in Appendix II. Finally, the specimens were also examined by microhardness gradient measurements, by electron microprobe analysis and by X-ray fluorescence analysis.

3. Results

In Table III the composition of the UC powder is given before annealing and also after an annealing treatment of 7oo hours at 7oo°C in contact with the capsule (type 43ol stainless steel) and 4 tensile test specimens. It is interesting to note that the equivalent carbon content of the UC remained unchanged and that the slight oxygen and nitrogen pickup during the anneal had released the equivalent amount of carbon for carburisation

of the capsule and specimens. This oxygen pickup (from 2oo to 7oo ppm) could arise from the reduction of thin oxide films on the steel capsules (the specimens had been electropolished) and secondly, as the nitrogen pickup from loo to 3oo ppm would indicate, from a slight ingress of air by diffusion trough the wall of the silica capsule during the annealing treatment in the furnace. In reality, therefore, all of these results should not be taken as arising from just slightly overstoichiometric UC but rather from a stoichiometry which is somewhat higher i.e. approaching values of 4.9 % equivalent carbon.

3.1 Steel 4988

In figs. 2, 3 and 4 the change in o.2 % yield strength, tensile strength and elongation are given for steel 4988 annealed in contact with UC. The curves obtained during annealing without UC are included for comparison purposes. It is clear that at all three temperatures the strength properties are significantly reduced whereas the ductility was not affected much by the annealing treatment in contact with UC. The magnitude of the strength reduction was the greatest at 7oo°C where the yield strength, after 11oo hours in contact with the UC, had dropped by as much as 3o %.

In fig. 5 the microhardness gradients from the surface to the interior of the specimens are given after 11oo hours in contact with UC at 6oo to 8oo°C. Somewhat surprisingly, a decrease in hardness was found near the edge of the specimens. The depth of this softer region was the least at 6oo°C and the greatest at 7oo°C. Similar microhardness gradients have also been found by Hofmann after annealing this steel in contact with UC of stoichiometry 4.9 % C [7].

Optical microstructural examinations did not reveal any signs of an interaction, and so, electron microscopy was used. In figs. 6 and 7 these microstructures, after 3oo hours at 6oo°C and 7oo hours at 7oo°C in contact with UC, are shown. The V(CN) phase appears as a fine thread-like precipitate at 6oo°C and as a small feathery-type precipitate at 7oo°C. The medium-sized precipitates are secondary NbC particles while the large isolated particles are primary (VNb)C particles or the $NbFe_2$ phase [5]. The structure at 8oo°C is very similar to that at 7oo°C and is not shown here. A comparison of the microstructure at the edge of the specimen to the normal microstructure in the center of the specimen did not reveal any new phases due to carburisation but did show quite clearly that the amount of the secondary NbC and also the V(CN) phase near the edge was considerably less than that in the normal structure. This effect is clearly to be seen in figs.6 and 7. After prolonged annealing in contact with UC these depleted regions reached depths of up to 1oo microns and this was confirmed by the microhardness gradients in fig. 5.

Quantitative volume fraction measurements were made on the NbC particles after each annealing treatment, as shown in fig. 8. Measurements on two specimens annealed in vacuum at 7oo°C show that his dissolution of the NbC phase near the edge of the specimen after annealing in contact with UC is not due to any prior fabrication treatment but is directly related to the close contact with the UC. The magnitude of this effect is quite large at 7oo and 8oo°C, with only about 3o % of the NbC phase

still remaining near the edge of the specimen after 1100 hours at 800°C. A similar effect is apparent with the V(CN) phase although the morphology of this phase did not make any quantitative volume fraction measurements possible. Electron diffraction analysis of remaining particles of these two phases near the edge of the specimen showed no change in crystal structure or lattice parameter from those found in the normal structure [5].

All these specimens were given the usual, for this material, prior solution treatment and an ageing treatment of 3 hours at 750°C, but this brief ageing treatment was not enough to prevent normal further precipitation and coarsening of the NbC and V(CN) phases upon further annealing at 600 to 800°C, as was shown under vacuum annealing conditions [5]. During an annealing treatment in contact with UC, therefore, an interaction could exist between the dissolution by the UC and the normal precipitation and coarsening behaviour caused by the thermal annealing treatment. To observe whether this would have an effect on the dissolution kinetics of the NbC particles during contact with the UC, some specimens were extensively annealed in vacuum prior to a further annealing treatment in UC, as shown in Table IV. This prior vacuum annealing treatment caused this normal precipitation behaviour to be fully completed before dissolution by the UC is started. In this same table the expected amount of dissolution without prior vacuum annealing treatment is given by interpolation from fig. 8. It is clear that the amount of dissolution of the NbC phase is less at all three temperatures if the normal precipitation behaviour is taken to completion before inserting the specimens into the UC.

Finally, X-ray fluorescence analysis from the specimen surfaces did not show any significant change in the Nb, V or Cr concentration near the edge of the specimen, as shown in Table V, and this was also confirmed by electron microprobe analysis. Also total carbon analysis did not reveal any significant carbon pickup by the specimens, also shown in Table V.

3.2 Incoloy 800: mill-annealed

The term "mill-annealed" is derived from the ASTM specification for Incoloy 800 after a recrystallisation heat treatment at 980°C. The room temperature mechanical properties of the mill-annealed structure upon annealing in UC and in vacuum respectively, are shown in figs. 9, 10 and 11. At 600°C a slight drop in yield and tensile strength is found upon annealing in contact with UC but the ductility was not affected measurably. At 700 and 800°C, however, the yield and tensile strengths remained unaffected by the UC but the ductility was reduced, this reduction in ductility being slightly greater at 700°C than at 800°C. In fig. 12 the microhardness gradients from the edge to the interior of the specimens are given after annealing for 1100 hours at 600 to 800°C in contact with UC. At 600°C no hardness gradient was found but at 700 and 800°C a noticeable hardening of the strcture had occurred to a depth of about 120 microns.

In figs. 12, 14 and 15 some of the corresponding microstructures are shown after annealing at 600, 700 and 800°C, respectively, in contact with UC. At 600°C the normal microstructure consists of $M_{23}C_6$ on the grain boundaries

and Ti(CN) particles dispersed troughout the grain interior. The annealing treatment in contact with the UC did not produce any new phases in the specimens except for a very thin film of $M_{23}C_6$ on the specimen surface, as shown in fig. 13. The twin grain boundaries are free from precipitates both near the edge of the specimen as well as in the center. At 700°C, however, extensive precipitation of $M_{23}C_6$ had occurred near the reaction interface and all boundaries, the high angle as well as the twin grain boundaries, have been covered by these precipitates and even some large sheet-like $M_{23}C_6$ precipitates occur in the grain interior, as shown in fig. 14. In the normal structure the twin grain boundaries are entirely free from any $M_{23}C_6$ precipitates and practically no, or only a few isolated, sheets of $M_{23}C_6$ are found within the grains. The Ti(CN) precipitates do not seem to be affected in any way by the presence of the UC next to the specimen. At 800°C, as shown in fig. 15, there is also extensive precipitation of $M_{23}C_6$ near the reaction interface but no twin grain boundaries are covered and no sheet-like $M_{23}C_6$ precipitates occur within the grains. As at 700°C, the Ti(CN) precipitates remained unaffected. These microstructural investigations confirmed the absence of a microhardness gradient at 600°C and the existence of one at 700 and 800°C.

3.3 Incoloy 800: solution treated

The room temperature mechanical properties of the solution treated structure upon annealing at 700 and 800°C in UC and in vacuum, respectively, are shown in figs. 16, 17 and 18 while in fig. 19 the microhardness gradients

are shown after 1100 hours at 700 and 800°C in contact with the UC. At both temperatures the yield strengths were very slightly reduced and the tensile strengths practically unaffected but, as in the mill-annealed condition, the ductility was reduced significantly by the annealing treatment in UC. Also the microhardness gradients show an increase in hardness near the reaction interface but, in this case, only to a depth of about 30 microns and not to such great depths as in the mill-annealed condition.

In fig. 20 some of the corresponding microstructures are shown. Once again the enhanced precipitation of $M_{23}C_6$ near the reaction interface is evident although this was not nearly as extensive as in the mill-annealed condition. At both temperatures some high angle grain boundaries containing no $M_{23}C_6$ can be seen in fig. 20. The $M_{23}C_6$ near the reaction interface occurred mainly in the form of sheet-like precipitates extending from a grain boundary into the grain interior and occurred only to a depth of about 50 microns from the edge of the specimen. In contrast to the alloy in the mill-annealed condition, however, an enhanced precipitation of TiC is evident near the reaction interface if compared to the normal structure in the center of the specimen.

3.4 Inconel 718

The room temperature mechanical properties of Inconel 718, solution treated and then annealed at 600 to 800°C in vacuum and in UC, respectively, are shown in figs. 21, 22 and 23 while in fig. 24 the microhardness gradients

from the edge to the interior of the specimens are shown after 1100 hours at 600 to 800°C in contact with the UC.

At 600°C the yield and tensile strengths are not affected significantly but the ductility is reduced to extremely low values after prolonged annealing in UC. The microhardness measurements also show an increase in hardness to a depth of about 60 microns after 1100 hours at 600°C in contact with the UC. At 700°C the yield and tensile strengths as well as the ductility are decreased after annealing in UC and a drop in hardness is found to a depth of about 30 microns from the edge of the specimen. At 800°C the yield strength is not affected much, the tensile strength is slightly reduced and the ductility very slightly increased by the treatment in UC while a drop in hardness, to a depth of about 60 microns, is also found near the edge of the specimen. It is clear that in this alloy the behaviour is very dependent on the temperature of annealing in UC.

The microstructures of this alloy, after annealing in UC for 1100 hours at 600, 700 and 800°C, are shown in figs. 25, 26 and 27 respectively. The normal microstructure at 600°C consists mainly of medium-sized M_6C particles, as shown in the bottom picture of fig. 25, and also the hardening phase which is a metastable body centered tetragonal phase of composition Ni_3 (NbAlTi). This phase is usually named γ' although it differs markedly from the normal fcc-γ' found in many other nickel-base alloys. This coherent bct-γ' precipitate is extremely fine at 600°C and is below the limit of resolution of carbon extraction replicas but can be easily resolved by thin foil electron microscopy [5]. Because of this, it was

not possible to observe the effect of the annealing treatment in UC on this hardening phase at 600°C. A very dense precipitation layer was, however, found at the surface, as shown in fig. 25. At 700°C these bct-γ' precipitates can be resolved and they are the small disc-shaped precipitates in the grain interior, as shown in fig. 26. In addition to this phase, the normal microstructure contains the larger angular M_6C particles, a thin film of NbC on the grain boundaries and, after 1100 hours at 700°C, the first traces of the very large disc-shaped stable precipitate which is the orthorhombic Ni_3Nb phase. This phase forms, upon overageing, from the metastable bct-γ' phase and the NbC on the grain boundaries [5]. The microstructure near the reaction interface with UC showed, first of all, also a dense layer of precipitates right at the surface of the specimen and secondly, that the bct-γ' phase had completely dissolved near the edge with some of the denuded regions extending up to 20 microns deep into the interior of the specimen. Furthermore, there is no sign of the stable Ni_3Nb phase near the edge of the specimen and the first traces of this transformation product were only found at depths greater than about 50 microns.

Finally, at 800°C, the normal structure consists of the stable Ni_3Nb phase with angular M_6C particles interspersed at random troughout the structure and the grain boundaries are free from the NbC films, as shown in fig. 27. Near the edge of the specimen there is, once again, a dense layer of precipitates, although these are much coarser at this temperature than at 600 or 700°C. Furthermore, the Ni_3Nb phase has been dissolved to appreciable depths and only after about 150 to 200 microns deep the normal microstructure

is found. Electron and X-ray diffraction analysis showed this dense layer of precipitates at the surface to consist of the M_6C phase with a lattice parameter of 11.05 Å. Electron microprobe analysis showed this phase to contain a fair amount of Cr, Nb, Mo and even a little Ti but no Ni, Fe or U.

4. Discussion

4.1 General

The extrapolation of these results to a real carbide fuel element is, understandably, of interest. The thickness of the specimens placed into the UC was about 0.90 mm (after electropolishing the originally 1 mm specimens) but, as these were in contact with the UC from both sides, the effects on the mechanical properties could roughly be the same as would occur in a real fuel element with a cladding thickness of about 0.4 to 0.5 mm and fuel on only one side. Secondly, the fuel densities were very low in these tests and in a real fuel element the degree of contact between fuel and cladding would be far greater, especially after some swelling had occurred, thereby enhancing any interaction by solid state diffusion. This does not necessarily apply to the carbon transfer from the fuel to the cladding, however, as the latter can occur by transport in the CO/CO_2 gas phase. The partial pressure of CO formed is proportional to the carbon activity in the fuel and the oxygen partial pressure and can lead to rates of carburisation which are essentially independent of the degree of close contact between the fuel and the cladding. This could be true in these tests as in no case was a point-selective carburisation of the specimens observed, as would have been the case if transfer had occurred only across the

points of contact between the fuel and cladding. In practice, where carbide fuels with an oxygen contamination are to be expected, the transfer of carbon across the gas-phase would probably also be the most significant mechanism of carburisation in fuel elements with no sodium-bonding. The CO can, therefore, play a role similar to the sodium in sodium-bonded fuel elements by increasing the kinetics of carbon transfer. Finally, the temperatures used in this investigation represent typical inner cladding temperatures as would occur in a real fuel element.

4.2 Steel 4988

Although examination by optical microscopy did not reveal any signs of an interaction between steel 4988 and the UC, the effects on the mechanical properties and the electron microscope investigations showed otherwise. The dissolution of the NbC and especially the V(CN) precipitates during the annealing treatment in UC, leads to very large reductions in the strength properties but, as no carburisation was found to occur, a likewise reduction in the ductility was not expected. The NbC volume fraction determinations in fig. 8 also indicate that the dissolution of these precipitates would probably continue beyond 1100 hours, making it likely that the strength properties would decrease even further upon prolonged annealing in contact with the UC.

The reason for the dissolution of the precipitates in the specimens is not quite clear as the experimental arrangement did not allow full investigation of the UC which had been in contact with the specimens of this steel. The most likely explanation, however, is that both Nb and V are depleted from the surface regions of the specimens by the

UC to form more stable mixed carbides in the fuel. This could be thermodynamically possible as VC is reported to be slightly and NbC completely soluble in UC at higher temperatures [8] and a slight solubility at lower temperatures could, therefore, exist. In the U-V-C system a second phase of composition UVC_2 does exist [9] but is not expected to form in this case as it does not occur if pure vanadium or its alloys are annealed in contact with UC [1o] and is, therefore, even less likely to be found here. The exact mechanism of the apparent Nb and V transfer from the cladding to the fuel cannot be established but it is significant that the amount of dissolution of NbC precipitates in the specimens is less if this phase is allowed to precipitate out fully and to coarsen before dissolution sets in. The relative high stability of NbC precipitates in steels is well known and these results indicate that the dissolution of the NbC precipitates could be rate-controlling in the entire transfer of Nb from the steel to the fuel.

Not quite clear is the lack of analytical evidence of a Nb or V depletion at the surface of the specimens. Calculations show that if 5o % of the NbC volume fraction is dissolved at the surface by the annealing treatment in UC, a decrease in total Nb content at the surface of about 1o % could result. Although the Nb analysis at 7oo°C in Table V would seem to confirm this figure, it is rather thought that this is not within the limits of detection by X-ray fluorescence analysis in this particular case.

4.3 Incoloy 8oo: mill-annealed

Incoloy 8oo is principally a solid solution hardened alloy and, consequently, the carbides usually found in this material ($M_{23}C_6$ and Ti(CN) normally do not contribute significantly to the strengthening of this alloy. Generally, the formation of $M_{23}C_6$ on grain boundaries, however, can lead to intergranular weakening, causing a reduction in ductility.

After annealing in contact with UC at 7oo and 8oo°C, the main reaction product in the cladding is an extensive formation of $M_{23}C_6$. As is to be expected, this does not affected the strength properties but does reduce the ductility significantly. At higher deformation temperatures, where intergranular fracture processes predominate, the reduction in ductility may be even greater. It is interesting to note the effect of different morphologies and nucleation sites of these newly formed $M_{23}C_6$ precipitates on the decrease in ductility. At 7oo°C, where these $M_{23}C_6$ precipitates near the edge of the specimen have nucleated as almost continuous films on all boundaries and even in the matrix in some cases, the elongation dropped from about 41 % to 35 %. At 8oo°C, however, where the newly formed $M_{23}C_6$ is much coarser, is discontinuous and is absent at the twin grain boundaries, the decrease in elongation is noticeably smaller than at 7oo°C. After annealing in contact with UC at 6oo°C, no fresh $M_{23}C_6$ is formed near the edge of the specimen and, consequently, no ductility decrease tue to the UC is found.

The slight drop in strength properties after annealing in UC at 600°C, however, cannot be explained satisfactorily. At temperatures below 620°C this particular alloy (with Ti = 0.32 %) can be strengthened [11] by the formation of pre-precipitation zones of γ'-Ni_3 (TiAl), as was found to occur under vaccum annealing conditions [5] in figs. 9 and 10. These zones are below the limit of resolution of the extraction replicas and cannot be seen in fig. 13. Somehow the formation of these strengthening zones must be affected by the annealing treatment in UC but it is difficult to specify this interaction further, especially as no microhardness gradient was found after annealing at this temperature. In general, the Ti(CN) precipitates do not play an active role in these alloys and also do not seem to be affected in any way by the treatment in UC.

4.4 Incoloy 800: solution treated

This alloy, in the solution treated condition, had very few twin grain boundaries, had a grain size about three times as large as in the mill-annealed condition and, upon vacuum annealing at 700 and 800°C, the Ti(CN) precipitate had a slightly larger lattice parameter and a different morphology than in the mill-annealed conditions [5]. Upon annealing in UC, the behaviour of this alloy in the solution treated condition also showed some distinct differences from that of the mill-annealed material.

At 700 and 800°C, after annealing in UC, a very slight decrease in yield strength occurred and, similarly to the mill-annealed material, no effect on the tensile strength but a significant effect on the ductility was found.

This decrease in ductility was, however, somewhat greater than in the mill-annealed condition at both temperatures. A further difference between the two initial conditions was the depth of penetration as seen by the microhardness gradients. In the solution treated condition the hardness increase was found only over a very shallow region while in the mill-annealed material this extended to depths almost 5 times as large.

The largest differences were observed in the microstructural behaviour. The extent of $M_{23}C_6$ precipitation, due to carburisation by the fuel, was much less in the solution treated condition than in the mill-annealed material. In spite of the much larger grain size of the solution treated material, which meant a much smaller grain boundary area per unit volume available for nucleation of $M_{23}C_6$, there were still a large number of high angle grain boundaries near the edge of the specimen which were entirely free from any $M_{23}C_6$, as shown in fig. 2o. This is in direct contrast to the mill-annealed condition where all grain boundaries near the edge of the specimen, especially at 7oo°C, are occupied by $M_{23}C_6$, as was shown in fig. 14.

Finally, in the solution treated condition, an enhanced precipitation of TiC was found near the edge of the specimen after annealing in contact with UC, whereas in the mill-annealed condition this does not occur. This indicates that during normal ageing after the solution treatment, the precipitation of Ti(CN) takes place only very slowly and may be limited by the low carbon content of this alloy, especially as this precipitate, in the solution treated material, was found to be a carbon-rich phase [5].

A small amount of Ti could, therefore, still be in solution to precipitate out as TiC near the edge of the specimen upon carburisation of the alloy by the UC. In the mill-annealed condition, however, this precipitate is a slightly nitrogen-rich precipitate [5] and during the recrystallisation treatment at 980°C a greater amount of Ti may be removed from solution as this alloy contains a relatively high amount of nitrogen. Less Ti would, therefore, be available in solution to precipitate out as TiC during carburisation of the cladding by the UC which, in turn, would mean a greater amount of $M_{23}C_6$, as was found to be the case. With TiC being more stable than $M_{23}C_6$, the former precipitates out preferably upon carburisation if Ti is still available in solution. The enhanced precipitation of TiC near the edge of the specimens in the solution treated material would not be expected to strengthen this alloy and the slight reduction in yield strength after annealing in UC could possibly be attributed to the enhanced removal of Cr and Ti from solid solution near the edge of the specimen.

In conclusion it can be stated that, although the penetration depths in the solution treated condition are less than in the mill-annealed condition, the ductility decrease is slightly greater in the solution treated condition. Judging from the compatibility point of view only, the mill-annealed condition should, therefore, be preferred.

4.5 Inconel 718

The behaviour of this alloy after annealing in contact with UC at 600°C is not well understood. It is quite obvious, however, that the use of this alloy as a cladding for UC fuel must be restricted because of the serious embrittlement that occurs at 600°C, where elongation values of only a few percent were found after 1100 hours in contact with UC.

The behaviour at 700 and 800°C, however, is more clear. At these two temperatures a niobium-containing M_6C precipitate is formed near the edge of the specimen at the expense of the niobium-containing precipitates in the normal structure. The dissolution of these niobium-containing precipitates in the matrix causes a reduction in the strength properties of up to 15 % at 700°C and also causes the drop in hardness near the edge of the specimen at 700 and 800°C. The dissolution of the stable Ni_3Nb phase at 800°C is less serious as this phase does not contribute much to the strengthening of this alloy and even causes a slight increase in ductility after prolonged annealing in contact with UC at 800°C.

Unfortunately, the exact composition of the M_6C phase that is formed in the cladding at the reaction interface, could not be determined although microprobe analysis showed it to contain Mo, Nb, Cr and a little Ti. The lattice parameter of 11.05 Å is less than that of the known [12] niobium-containing M_6C precipitates of Cr_3Nb_3C (a= 11.49 Å), $(VNi)_3Nb_3C$ (a = 11.50 Å) and $Ni_2(TiNb)_4C$ (a = 11.58 Å) although the latter two are excluded in any case because of their Ni contents. The Ni-depletion in this 20 to 30 microns layer is probably due to the formation of UNi_5 in the fuel, a reaction product which is quite common with high nickel or nickel-base alloys [13]. Because this latter reaction must necessarily involve solid state diffusion, a localised attack, which is confined only to those points of contact between the UC particles and the cladding, is expected. This probably caused the surface roughness of the reaction interface of this alloy at 700 and 800°C, as seen in figs. 26 and 27. Such a surface roughness was not found in steel 4988 and only to small extent in Incoloy 800.

5. Conclusions

5.1 Steel 4988

1. The strength properties are reduced considerably by the annealing treatment in UC at all three temperatures.
2. No carburisation of the specimens was found to occur and, hence, the ductility remained unaffected.
3. The NbC and V(CN) phases were found to dissolve in the specimens near the reaction interface causing the observed reductions in mechanical strength and a decrease in hardness near the surface of the specimens.
4. The amount of dissolution of the NbC phase is less if this phase is allowed to precipitate out fully and to coarsen before the dissolution by the UC sets in.

5.2 Incoloy 800: mill-annealed

1. At 600°C the normal strengthening, due to pre-precipitation zone formation, does not take place during annealing in contact with the UC. The reason for this is not quite clear.
2. No extra $M_{23}C_6$, due to carburisation by the UC, is found at 600°C and, consequently, the ductility remains unaffected.
3. At 700 and 800°C extensive precipitation of $M_{23}C_6$ occurs due to carburisation by the UC. This does not affect the strength properties but decreases the ductility noticeably.
4. The Ti(CN) phase in this material does not seem to be affected in any way by the annealing treatment in UC.

5.3 Incoloy 800: solution treated

1. The extent of $M_{23}C_6$ formation in this material was much less than in the mill-annealed condition upon annealing in contact with UC.
2. An enhanced precipitation of TiC is found near the edge of the specimens in contact with UC but this does not seem to affect the strength properties much.
3. A ductility decrease occurs due to carburisation at 700 and 800°C. This decrease is greater than in the mill-annealed material.

5.5 Inconel 718

1. At 600°C the strengt properties are not affected by annealing in contact with UC but the ductility is reduced to very low values.
2. At 700 and 800°C the strength properties are reduced and the ductility is decreased at 700°C and increased slightly at 800°C by annealing in contact with UC.
3. At all three temperatures a dense layer of M_6C is formed at the surface of the specimens. This phase contains Mo, Cr, Nb and a little Ti but not Fe, Ni or U. This niobium-containing M_6C forms at the expense of the strengthening phase, bct-γ' (Ni_3 (NbAlTi)) at 700°C and of the stable orthorhombic Ni_3Nb phase at 800°C.
4. A nickel-depletion, probably due to the formation of UNi_5 in the fuel, also occurs near the edge of the specimen in contact with the UC at 700 and 800°C.

Acknowledgements

We would like to thank Mr. Strömann for the microprobe analysis, Dr. W. Schneider for the X-ray diffraction analysis and Dr. (Mrs.) H. Schneider for the chemical analyses. One of us (W.E.S.) would like to thank the South African Atomic Energy Board for the financial support while at the Karlsruhe Nuclear Research Center.

Appendix I

The preparation of carbon extraction replicas from precipitation zones near the edge of a specimen

The use of carbon extraction replicas for the general microstructural examination of precipitation hardenable materials has been well documented. Especially for the carbide precipitation behaviour in steels, this technique has been used extensively in the past. This is mainly due to the ease of preparation (if compared to the preparation of thin films), the high resolving power (generally as high as 2o to 5o Å) and the fact that very large areas of the specimen are available for examination. A further advantage of this technique is that the precipitates are extracted and are available in the electron microscope for electron diffraction analysis.

The study of the precipitation behaviour near the edge of a polished specimen has, however, always been hampered by the fact that the carbon film, which is only a few hundred Ångstrom thick, usually tears and breaks up near the edge of the specimen as it is not fully supported

by the grids of the electron microscope grid-support in this region. To prevent this, one would have to extend the carbon film well beyond the edge of the specimen so that the tearing and breaking of the film takes place in this extended region and not in the film at the edge of the specimen. Because the carbon film, after evaporation onto the specimen, has to be etched loose, such an extension of the carbon film beyond the edge of the specimen can only take place on a metallic substrate. Consequently, electroplating of the specimens with nickel was considered for this purpose. For the breaking up of the carbon film to take place entirely in the extended region of the film, the film would have to extend over at least the grid-spacing of the electron microscope grids. This meant that the electroplated layer had to be at least 8o microns thick as the grid-spacing of type 2oo grids was of this order. A second prerequisite of the electroplating was that the tight adherence of the electroplating to the specimen was of utmost importance. If this could not be maintained during the subsequent mounting, grinding, polishing and etching of the specimen, the carbon film would part a the nickel-specimen interface, leaving the carbon film at the edge of the specimen once again unsupported. This latter requirement proved to be extremely difficult to meet and considerable time was spent in selecting the best electroplating procedure.

Specimen treatment prior to electroplating

For proper adherence of the electroplated layer to the specimen the surface preparation of the specimen is of importance. First of all, the specimen was degreased in an ultrasonic acetone bath for lo minutes and was then etched electrolytically in a lo % oxalic acid bath at about 5 volts. This etching time was kept very short

(a few seconds) in order not to etch away any of the reaction products in the specimen which were to be studied. The specimen was then once again cleaned in acetone and finally washed in distilled water before being placed in the electroplating bath.

Electroplating bath

The electroplating bath which was used, has been described by Samuels [14]. Briefly, it consists of 3oo gm/l $NiSo_4$, 6o gm/l $NiCl_2$, and 4o gm/l H_3BO_3. The pH of this solution should be about 4. To this is added 1 part of 3o % H_2O_2 per 2oo parts of solution once a day. The temperature of the bath was kept at 5o^{o}C and the bath was stirred vigorously during electroplating. The anode consisted of a 99.9 % nickel sheet in a cloth bag, the latter being necessary to prevent the brown anode deposit from entering the solution. For proper adherence of the electroplated layer to the surface, the current density was kept very low i.e. 2o to 3o mA/cm^2. Unfortunately this requires very long plating times-about 3 to 4 hours for a plating of 8o microns thick. Finally, a fresh solution had to be made up after the plating of about 15 to 2o specimens, which corresponds to a total electroplated area of about 4o to 6o cm^2.

Metallographic preparation

The metallographic preparation of the specimens was found to have an effect on the final adherence of the

plating to the specimen. In the first place, harder mounting materials mounted under pressure, like Bakelite, were found to be superior to the softer ones as the latter materials can deform more easily during grinding, thereby not supporting the nickel plating firmly onto the specimen. Secondly, the coarse grinding of the specimen had to be carried out parallel to the electroplated edge of the specimen and not across it. Once the polishing stages had been reached, however, the direction of polishing could be chosen at will. Finally, the carbon extraction replicas were prepared across the specimen plus electroplating as described elsewhere [5, 6].

In spite of these precautions, however, a large proportion of the final replicas had parted at the electroplating to specimen surface interface, making it necessary to repeat the whole procedure.

Appendix II

The determination of the volume fraction ratio f_v (edge)/f_v (center) for the NbC phase in steel 4988

The volume fraction of a second phase can be determined from an extraction replica by the formula [15]

$$f_v = \frac{\pi}{6} N_s \left(\bar{x}_{Ai}^2 + \sigma_{Ai}^2\right)$$

where f_v is the volume fraction, N_s is the number of particles per unit area, $\bar{x}_{Ai}$ is the mean particle

diameter of an arithmatic area distribution and σ_{Ai} is the standard deviation of the same distribution. In some previous work [16] it was shown, however, that this formula can only yield accurate volume fractions under the following conditions:

(a) the factor $(\bar{x}_{A_i}^2 + \sigma_{A_i}^2)$ will only be accurate if the replica is prepared after a very deep initial etch as all sectioned particles (from polishing) have to be eliminated. This etching depth should be greater than the radius of the largest particle in the distribution.

(b) The factor N_S can only be determined accurately if the initial etching depth is kept extremely shallow as deep etching causes severe surface roughness and hence an increase in true surface area although the projected area may remain constant.

As these two requirements are mutually exclusive it was shown that accurate volume fractions can only be determined from the above formula if two replicas are prepared. The one, after deep initial etching, for the determination of $(\bar{x}_{A_i}^2 + \sigma_{A_i}^2)$ and the second, after no etching or only a very shallow etch, for the determination of N_S.

As the double replica technique is quite tedious if a large number of volume fraction determinations are required, the change in volume fraction of the NbC phase near the edge of the specimen of steel 4988 was expressed

as a ratio to the volume fraction in the center of the specimen i.e. the normal volume fraction. This requires the preparation of only one replica as the following argument proves.

If a replica is prepared from the specimen after a very deep initial etch, the volume fraction formulas can be written as follows

$$f_V(\text{Edge}) = \frac{\pi}{6}\left(\frac{N_E}{A_E \alpha_E}\right)\left(\bar{x}_{A_1}^2 + \sigma_{A_1}^2\right)_E$$

and

$$f_V(\text{center}) = \frac{\pi}{6}\left(\frac{N_C}{A_C \alpha_C}\right)\left(\bar{x}_{A_1}^2 + \sigma_{A_1}^2\right)_C$$

In these formulas the subscripts E and C refer to the edge and the center of the specimen respectively. Here N is the number of particles counted on the projected area A and α is an unknown surface roughness factor introduced by the deep initial etch. This factor can be substantially higher than one, even approaching values as high as two. It is only when the initial etching depth is kept extremely shallow that this factor approaches one [6, 16].

If the volume fractions at the edge and center of the specimen are determined on the same replica, however, it can be assumed that $\alpha_E = \alpha_C$ as the edge and center of the specimen were subjected to exactly the same etching procedure. By expressing the volume fractions

as a ratio these unknown surface roughness factors are cancelled and all other factors in the above formulas can be determined quite accurately from the deeply etched specimen.

A further advantage of expressing the volume fraction at the edge of the specimen as a ratio to the normal volume fraction in the center of the specimen, is that any normal changes in volume fraction due to the annealing treatment are not reflected in the final figure but only the change in volume fraction caused by the UC near the edge (or surface) of the specimen.

References

[1] P.E. Elkins, "Compatibility of uranium carbide fuels with cladding materials", NAA-SR-7502, August 1964

[2] R. Pascard, "Properties of carbides and carbonitrides" from "Plutonium Fuel Technology", Met. Soc. AIME (Nucl. Mat.) 13 (1968) 345

[3] A. Thorley, B. Longson and J. Prescott, "Effect of exposure to sodium on the mechanical properties and structure of some ferritic, austenitic and high nickel alloys", TRG Report 1909 (C) 1970

[4] K. Goldmann, "Enviromental design factors for sodium-cooled fast reactor components", Paper IAEA/SM-130/62 at the IAEA Symp. on progress in Sodium-cooled Fast Reactor Engineering, held at Monaco 23 to 27 March, 1970

[5] W.E. Stumpf, "Room temperature tensile properties and microstructures of steel X8CrNiMoVNb 1613 (4988), Incoloy 800 and Inconel 718 after ageing at 600 to 800°C", KFK-1318, November 1970

[6] T. Mukherjee, W.E. Stumpf and C.M. Sellars, "Quantitative assessment of extraction replicas for particle analysis", Journ. of Mat. Science 3 (1968) 127

[7] P. Hofmann, Personal communication, GfK Karlsruhe, 1971

[8] H. Nowotny, R. Kieffer, F. Benesovsky and E. Laube, Monatsh. Chem., 88 (1957) 336

[9] F. Gorle, W. Timmermans, F. Casteels, J. Vangeel and M. Brabers, "Thermodynamics of Nuclear Materials", Proc. Symp. (Vienna, 1967) p. 481

[1o] O. Götzmann, P. Hofmann, W.E. Stumpf, "Verträglichkeitsuntersuchungen von Urankarbid mit Stählen und Vanadinlegierungen", Paper presented at the "International Meeting on Fast Reactor Fuel and Fuel Elements" held at Karlsruhe, 28-3o Sept., 197o

[11] C.N. Sparlaris, "Incoloy 8oo for nuclear fuel sheaths (a monograph)", GEAP-4633, July 1964

[12] W.B. Pearson, "A Handbook of Lattice Spacings and Structures of Metals and Alloys", Pergamon Press, Oxford 1958

[13] O. Götzmann and D. Scherbl, "Verträglichkeitsuntersuchungen mit UC verschiedener Stöchiometrie und Eisen-Nickel-Chrom-Legierungen und der Einfluß von Stabilisatoren", KFK-1213, Juni 197o

[14] L.E. Samuels, "Metallographic Polishing by Mechanical Methods", Publ. Pitman and Sons Ltd., London, p.164

[15] M.F. Ashby and R.B. Ebeling, "On the determination of the number, size spacing and volume fraction of spherical second-phase particles from extraction replicas", Trans. AIME 236 (1966) 1396

[16] W.E. Stumpf and C.M. Sellars, "Measurement of particle density and volume fraction from extraction replicas", Metallography 1 (1968) 25

Table I Composition of the alloys (wt %)

Alloy Melt No.	C	Cr	Ni	Mo	V	Nb	Ti	Al
4988 M166/66	0.08	16.1	13.6	1.30	0.75	0.87		
Incoloy 800 M209/68	0.03	20.5	31.6	0.05			0.32	0.40
Inconel 718 M167/66	0.04	18.8	52.5	3.0		5.0	0.90	0.50

N	Si	Mn	P	S	Co	Cu	Ta	B
0.10	0.29	1.10	0.19	0.10	0.05	0.05		1-2 ppm
0.06	0.46	0.67	0.006	0.003	0.10	0.10		2-3 ppm
	0.30	0.19	0.005	0.005	0.05	0.04	0.13	6 ppm

Table II Initial heat treatments and resulting grain size

Alloy	Heat treatment	Grain size (microns)
4988 aged	1050°C for 1 hr-WQ, aged 750°C for 3 hrs-AC	8
Incoloy 800 mill-annealed	980°C for 1 hr-WQ	14
Incoloy 800 solution treated	1150°C for 1 hr-WQ	42
Inconel 718 solution treated	980°C for 1 hr-AC	11

Table III Composition of UC before and after annealing (In ground condition: size fraction 25-63 microns). (in wt %)

	C	O	N	$C_{eg.}$
Before annealing	4.81	o.o71	o.oo9	4.84
After a compatibility anneal of 7oo hrs at 7oo°C in contact with steel capsule and specimens	4.77	o.o7	o.o3	4.85

Table IV Effect of pre-treatment on the dissolution of the NbC particles in Steel 4988 after annealing in contact with UC

	Treatment **	Vol.Fraction (edge) / Vol.Fraction (center)
a	7oo hrs 6oo°C in vacuum and then 5oo hrs 6oo°C in UC	o.893
b	Only 5oo hrs 6oo°C in UC	o.85o*
c	7oo hrs 7oo°C in vacuum and then 5oo hrs 7oo°C in UC	o.728
d	only 5oo hrs 7oo°C in UC	o.68o*
e	7oo hrs 8oo°C in vacuum and then 5oo hrs 8oo°C in UC	o.6o5
f	only 5oo hrs 8oo°C in UC	o.5oo*

* These are values taken from fig. 8

** All the specimens were initially given the normal solution treatment plus 3 hrs at 75o°C.

Table V X-ray fluorescence analysis* of Nb, V and Cr from specimen surfaces and also total carbon analysis after annealing steel 4988 in vacuum and in UC.

Treatment	Counts Nb/Fe	Counts V/Fe	Counts Cr/Fe	wt%C
1100 hrs at 700°C in vacuum	0.058	0.0045	0.185	0.082
1100 hrs at 700°C in UC	0.054	0.0042	0.19	0.080
1100 hrs at 800°C in vacuum	0.053	0.0043	0.192	0.084
1100 hrs at 800°C in UC	0.054	0.0042	0.188	0.079

* The concentrations of Nb, V and Cr are given as relative number of counts to Fe.

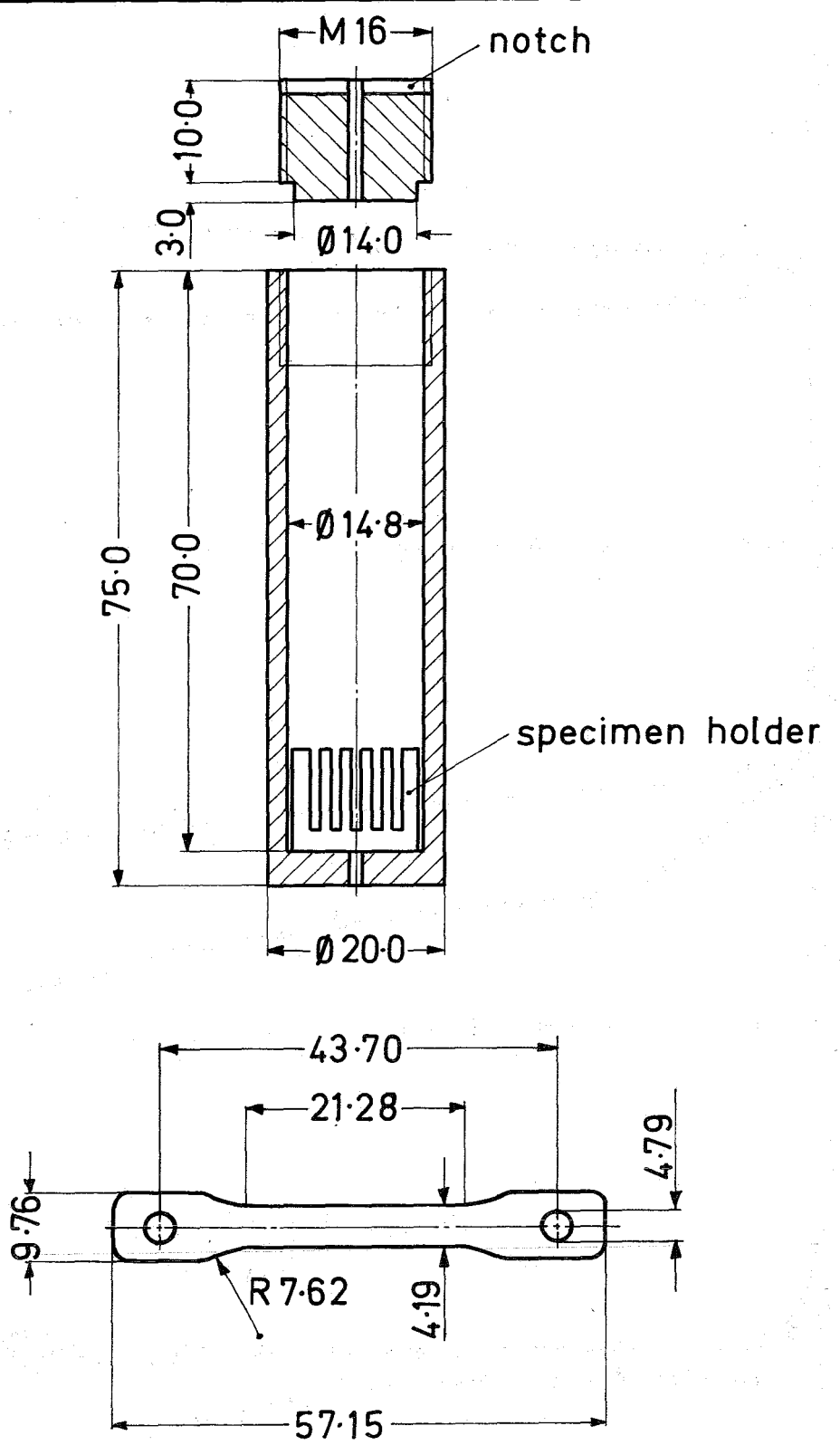

Compatibility capsule for annealing five tensile sheet specimens in UC powder.

FIG. 1

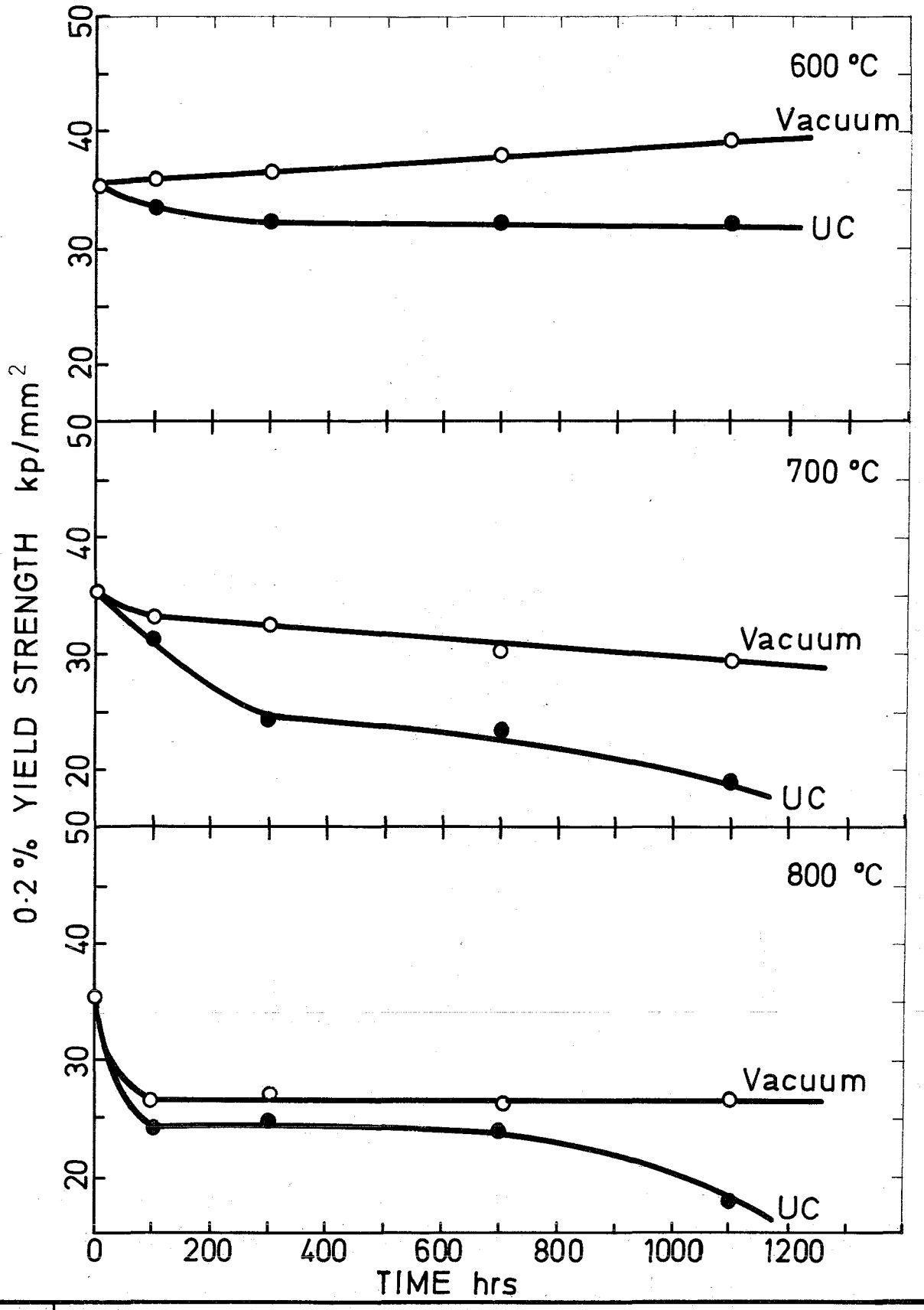

FIG. 2 Room temperature yield strength of STEEL 4988, solution treated and aged 3hrs and 750 °C and then annealed in vacuum(—o—) and in contact with UC (—●—)

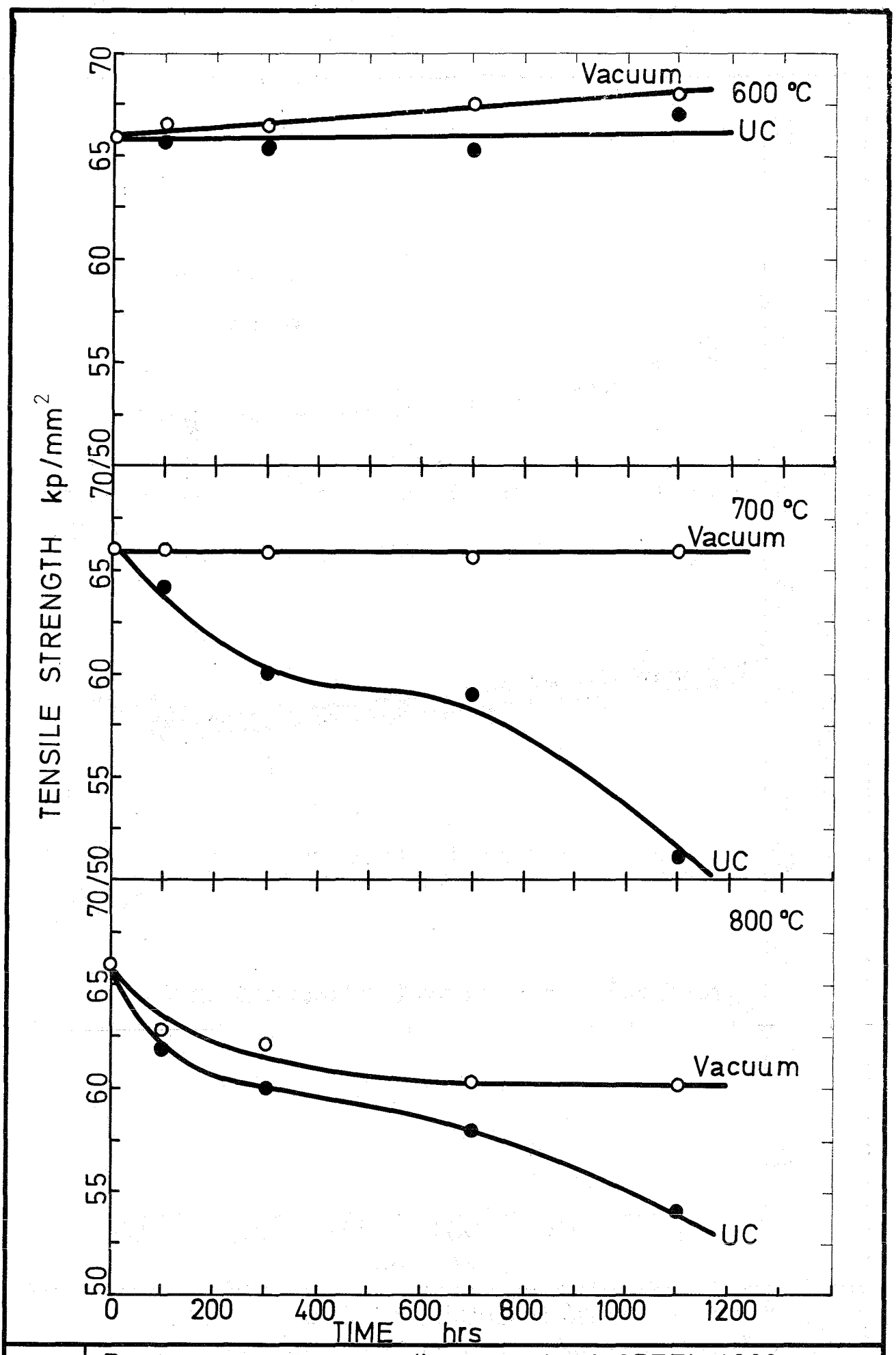

FIG. 3 Room temperature tensile strength of STEEL 4988, solution treated and aged 3hrs at 750 °C and then annealed in vacuum (—o—) and in contact with UC (—●—)

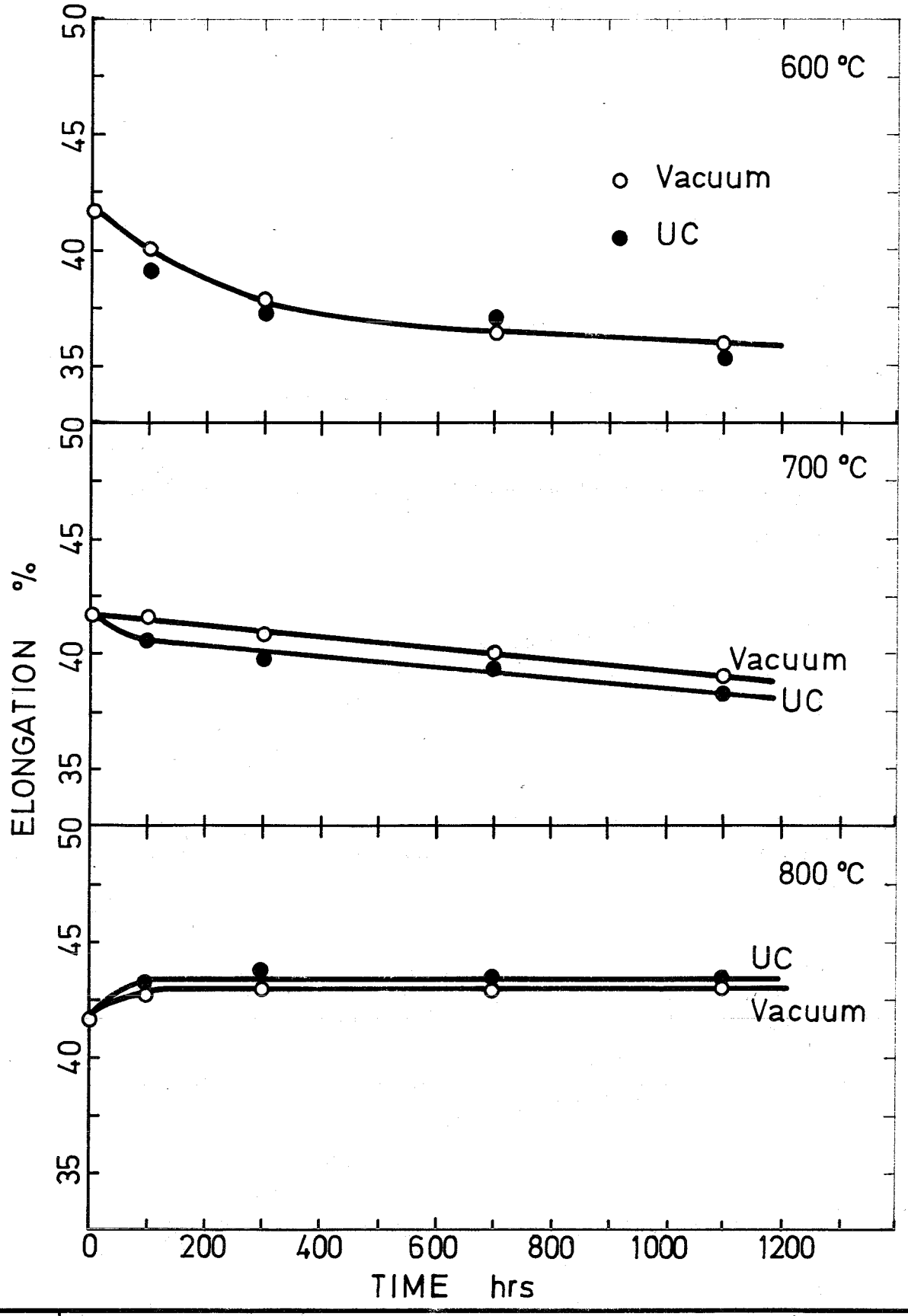

FIG. 4 Room temperature ductility of STEEL 4988, solution treated and aged 3 hrs at 750 °C and then annealed in vacuum (—o—) and in contact with UC (—●—)

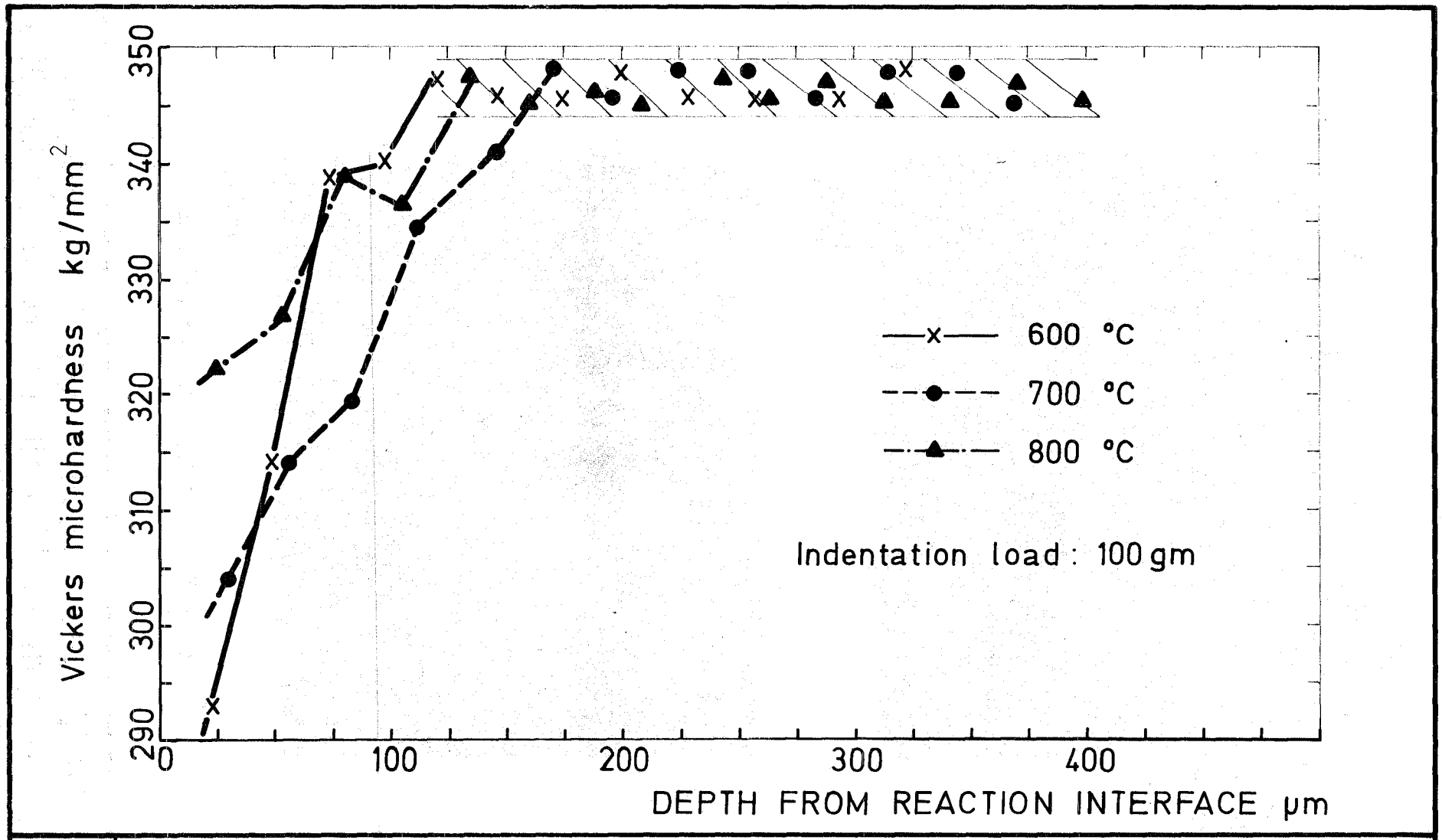

FIG. 5

Microhardness gradients in STEEL 4988, solution treated and aged 3 hrs at 750 °C before annealing further for 1100 h at 600, 700 and 800 °C in contact with UC.

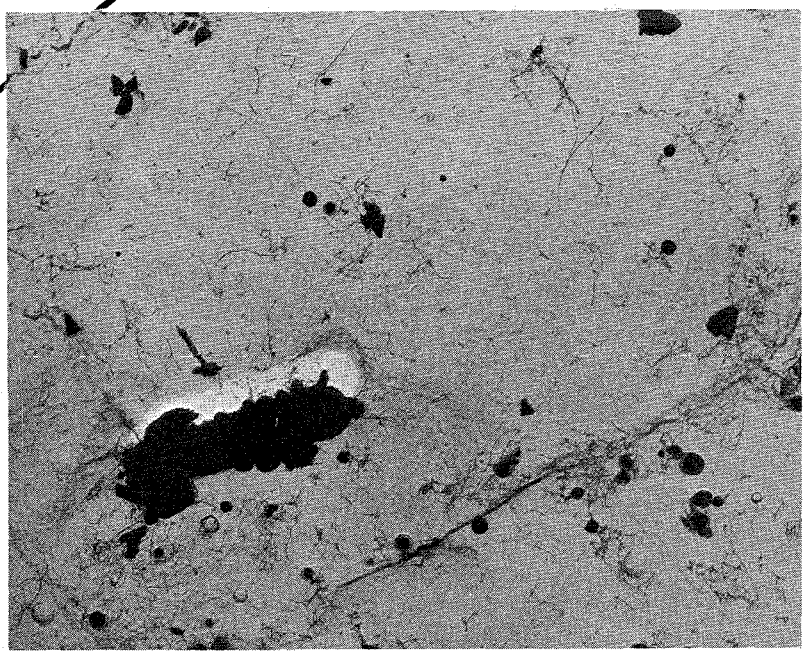

1µm

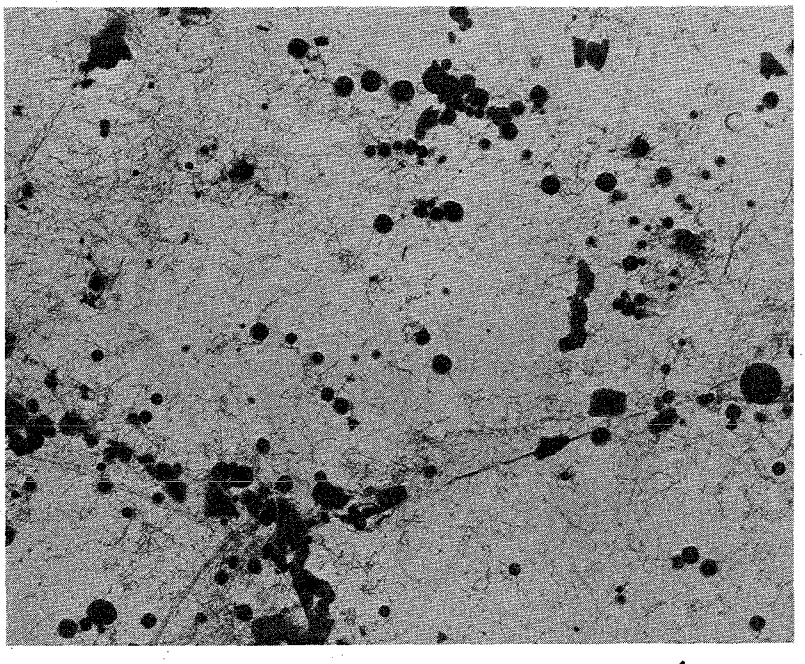

1µm

~500 µm from reaction interface

FIG. 6

STEEL 4988 solution treated and aged for 3 hrs at 750°C and then annealed for 300 hrs at 600°C in contact with UC

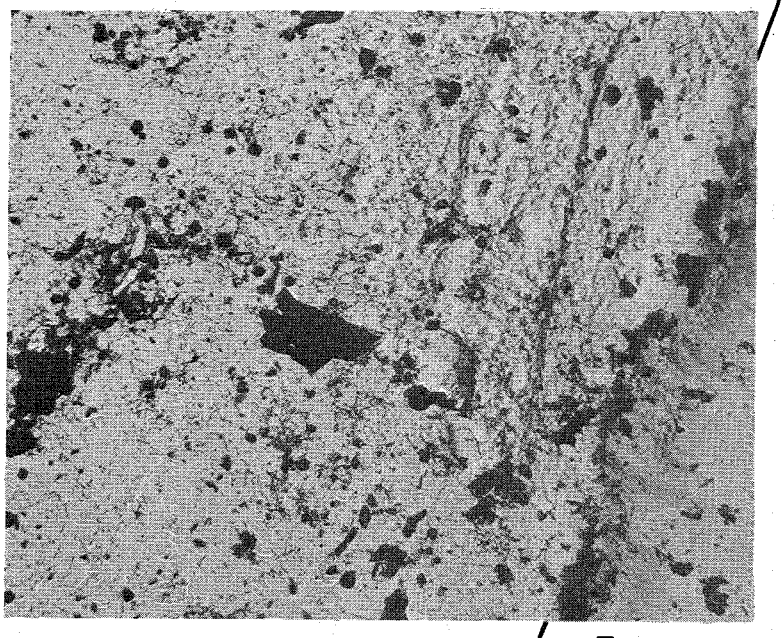

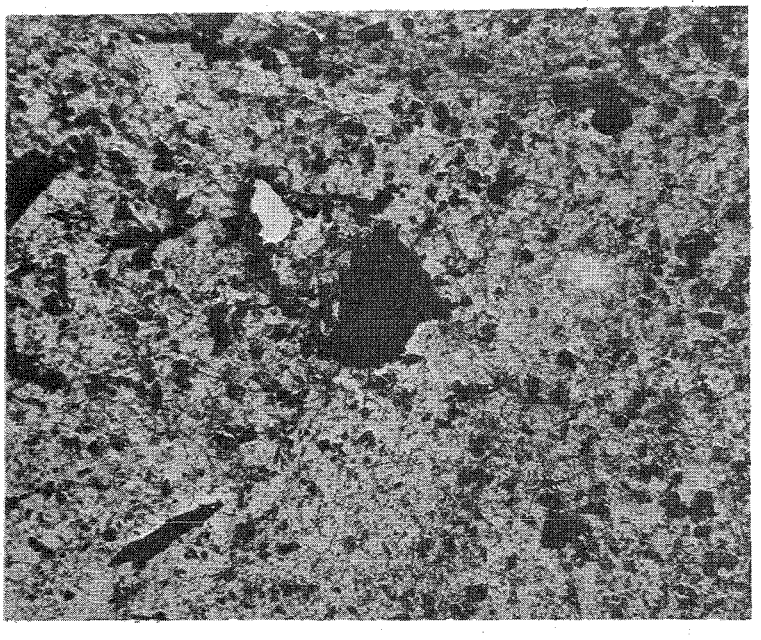

~500μm from reaction interface

FIG. 7

STEEL 4988 solution treated and aged for 3 hrs at 750°C and then annealed for 700 hrs at 700°C in contact with UC

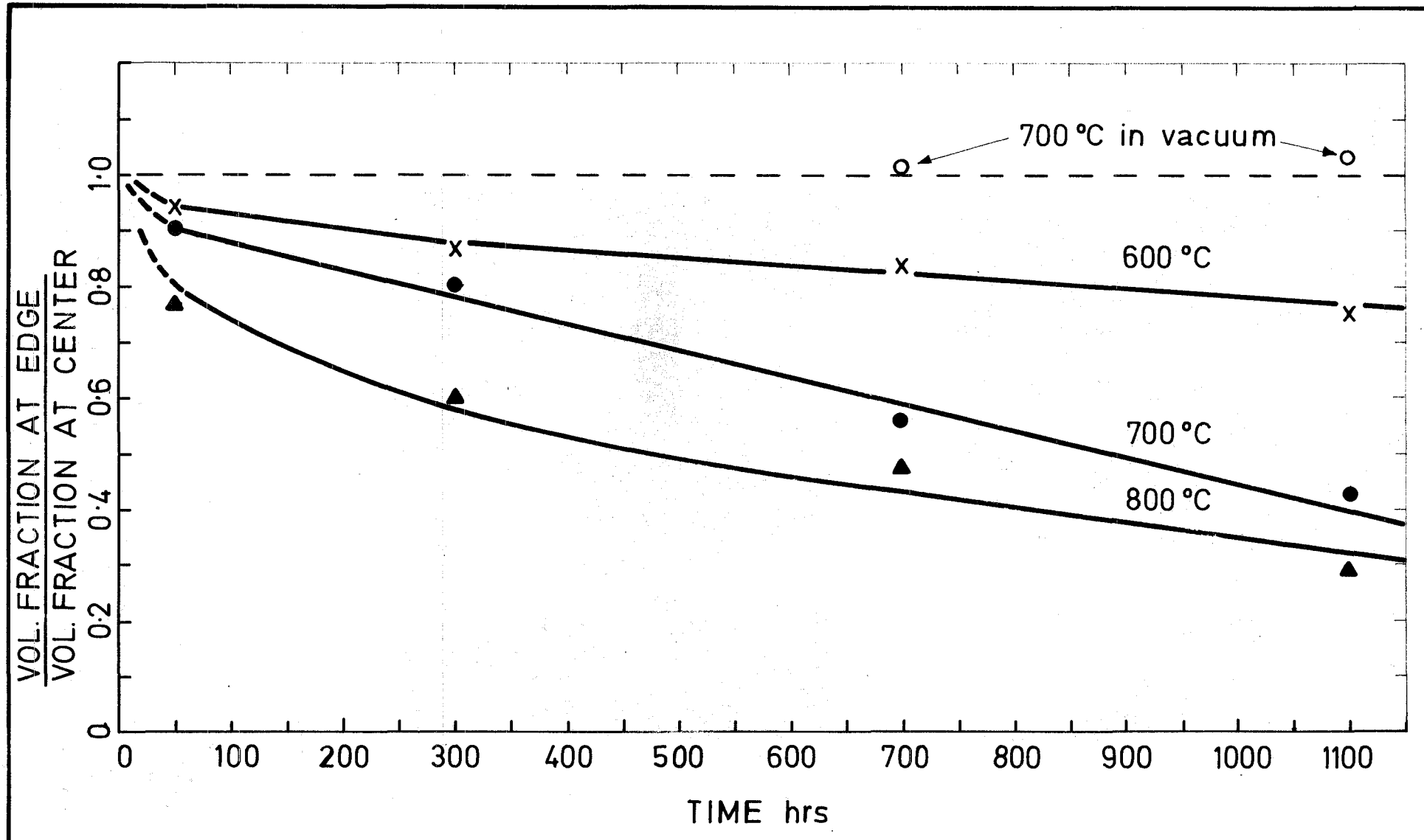

FIG. 8

STEEL 4988 Showing dissolution of NbC particles near the reaction interface after annealing in contact with UC

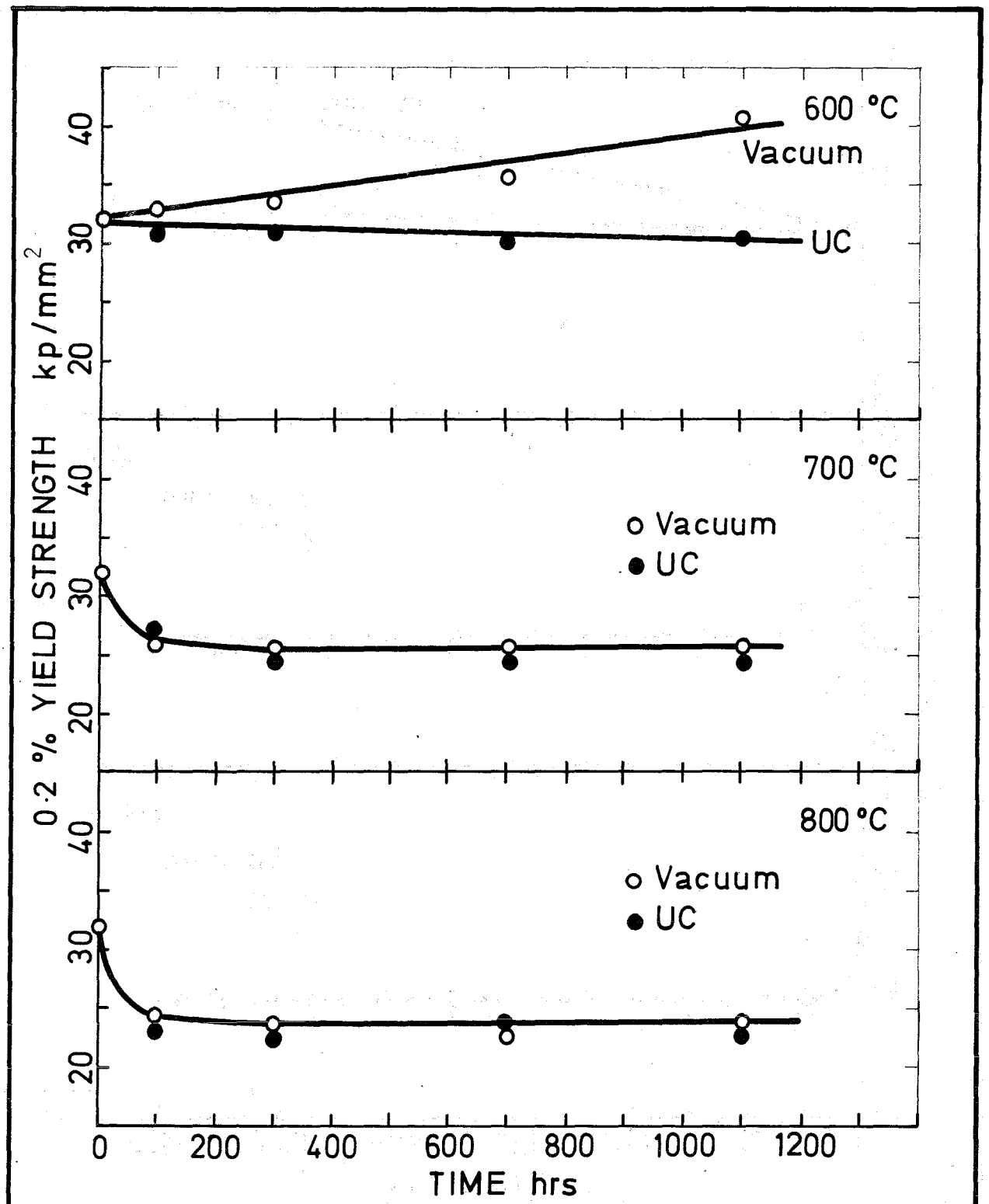

FIG. 9 Room temperature yield strength of INCOLOY 800, mill-annealed and annealed further in vacuum (—o—) and in contact with UC (—●—)

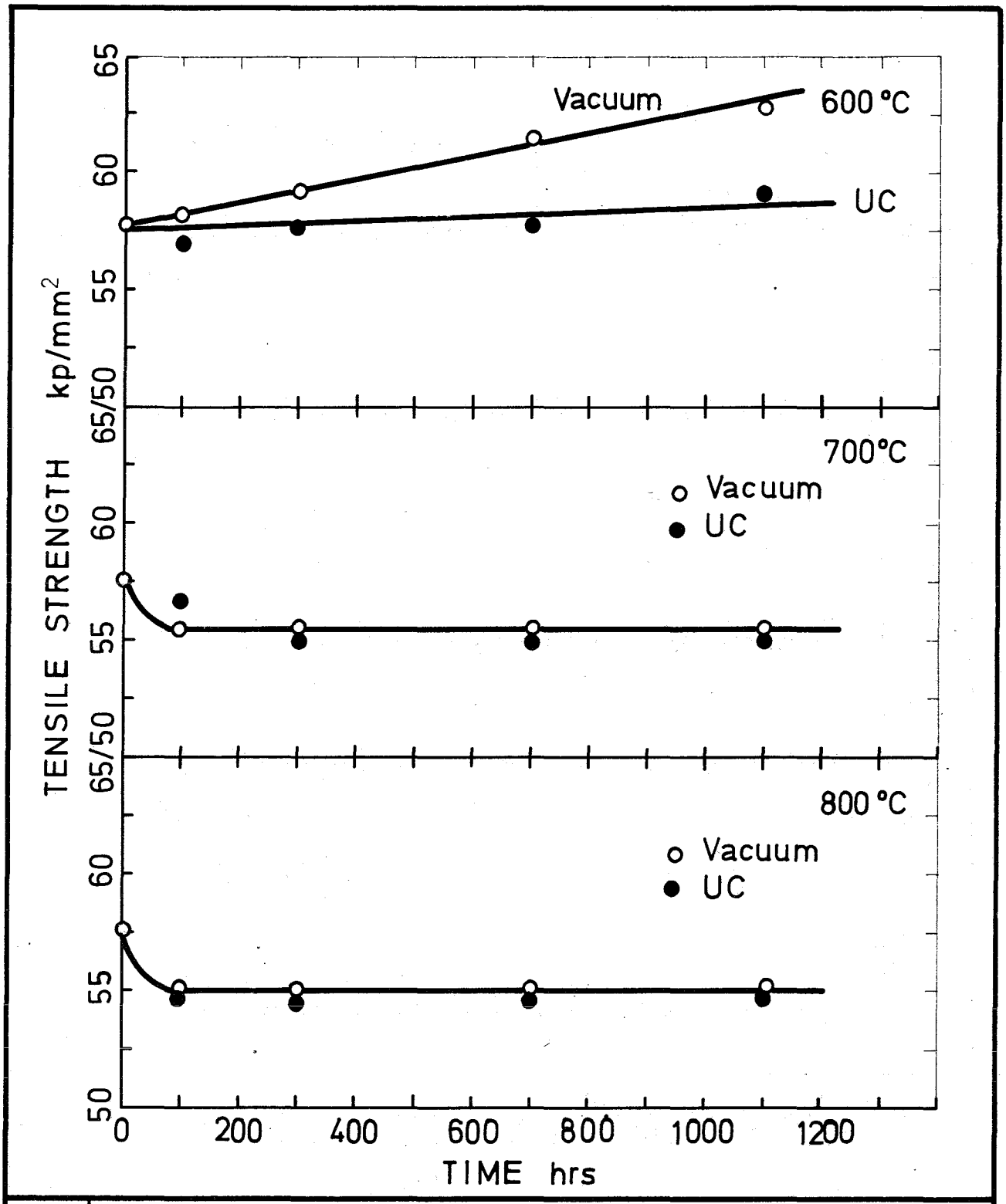

FIG. 10 Room temperature tensile strength of INCOLOY 800, mill-annealed and annealed further in vacuum (—o—) and in contact with UC (—●—)

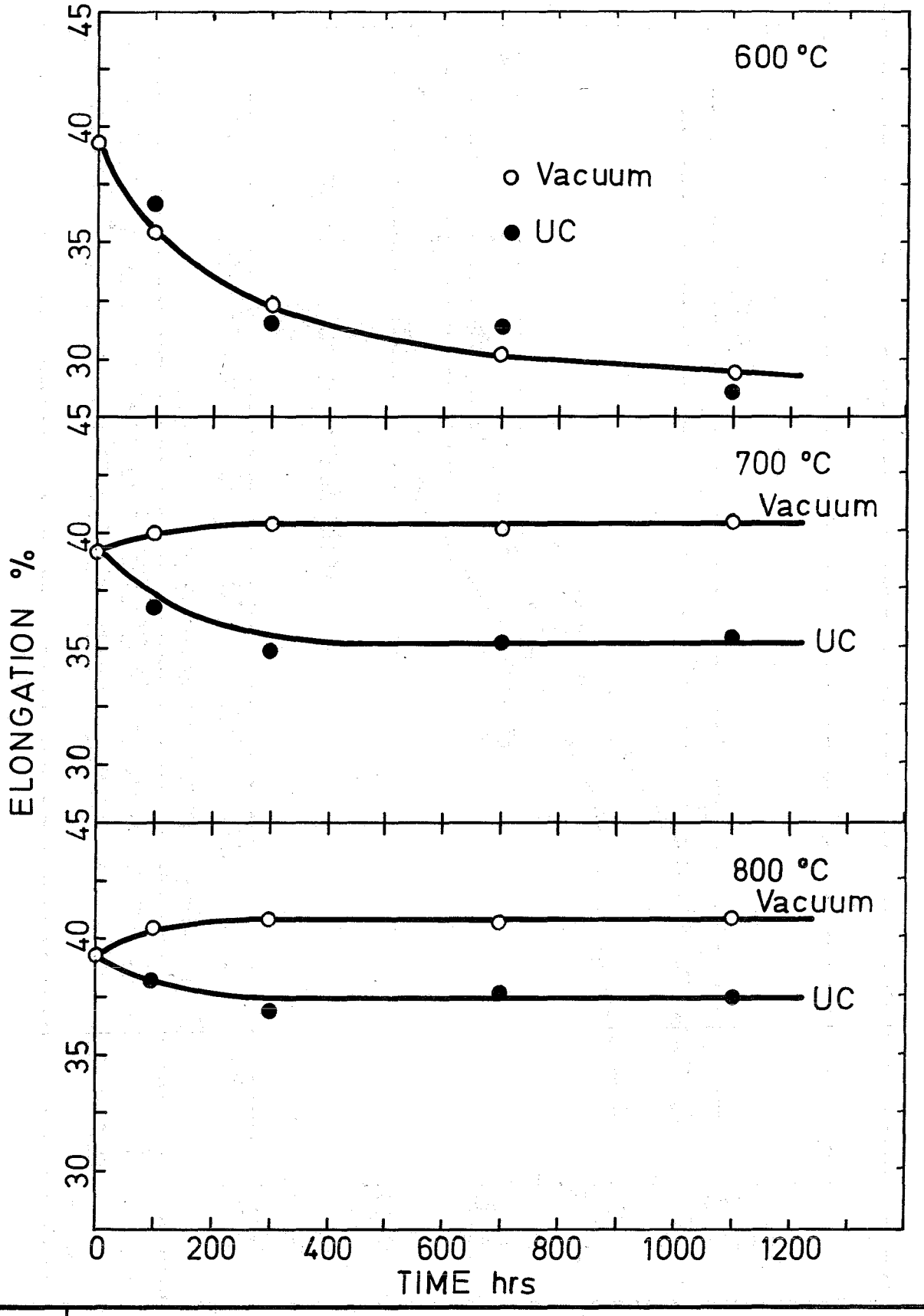

FIG. 11 Room temperature ductility of INCOLOY 800 mill-annealed and then annealed further in vacuum (—o—) and in contact with UC(—●—)

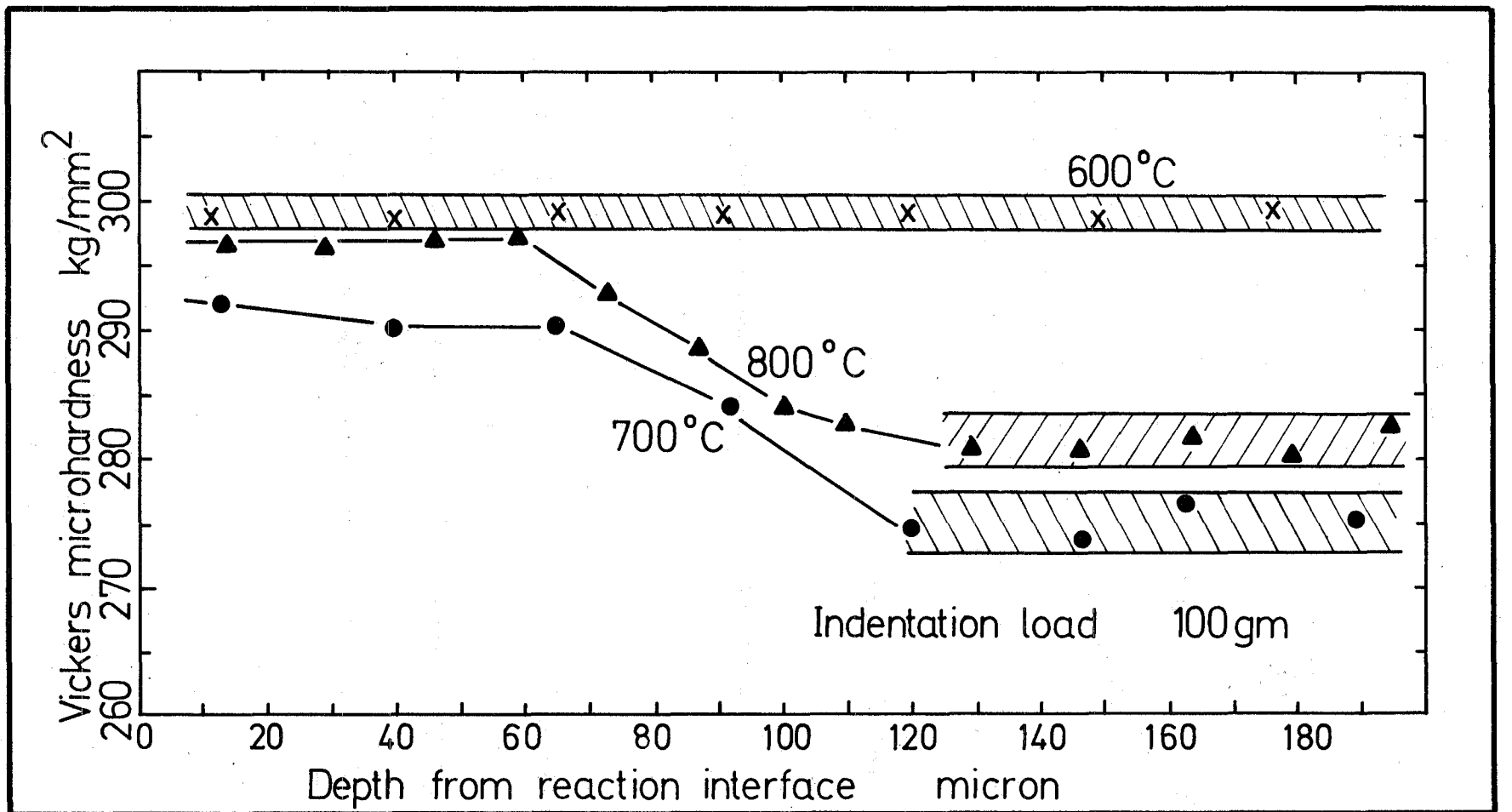

FIG. 12 Microhardness gradients in INCOLOY 800 mill-annealed and then annealed further in contact with UC for 1100 hrs at 600, 700 and 800°C.

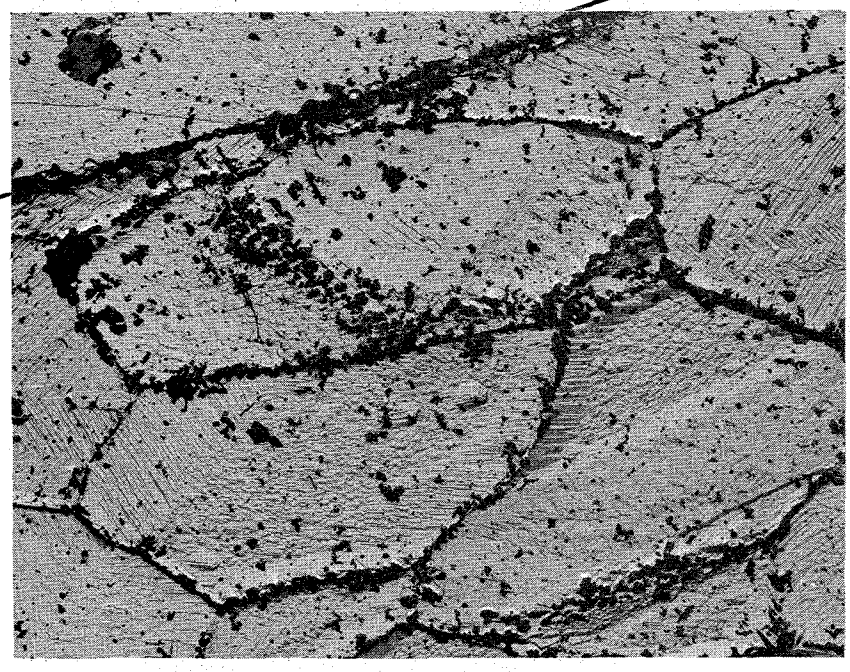

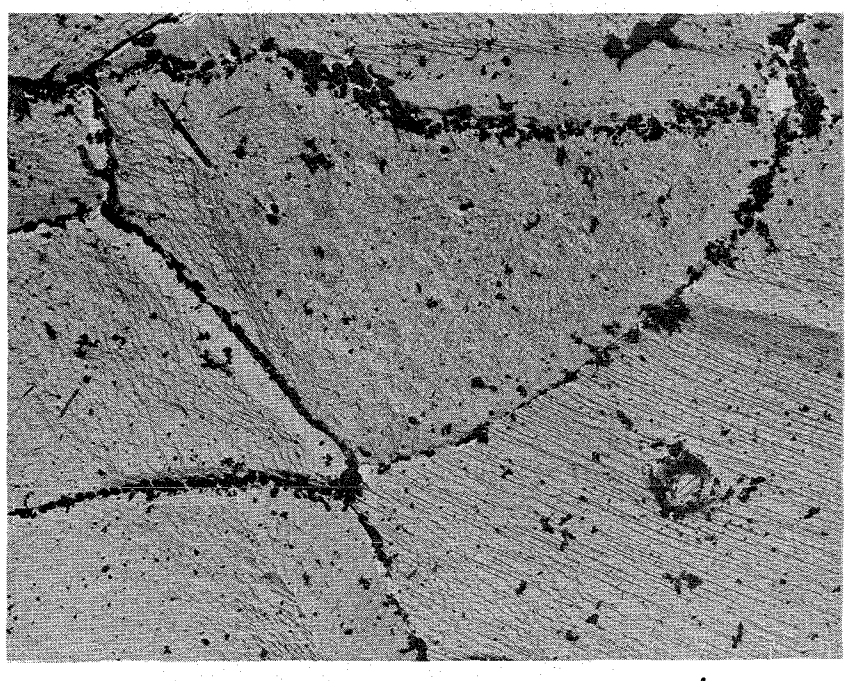

~ 500 µm from reaction interface

FIG. 13	INCOLOY 800 mill-annealed and then annealed further for 1100 hrs at 600°C in contact with UC

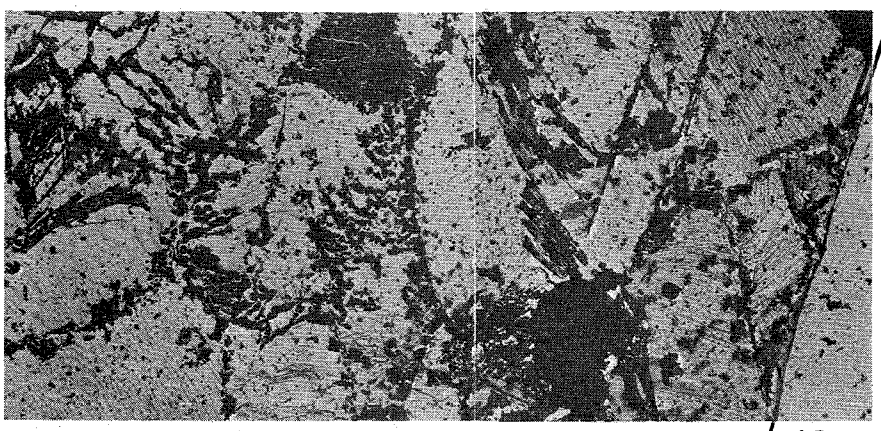

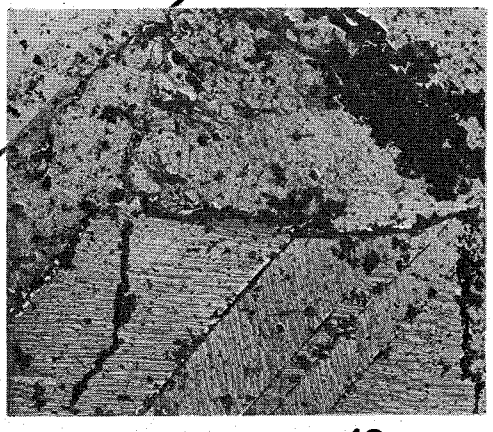

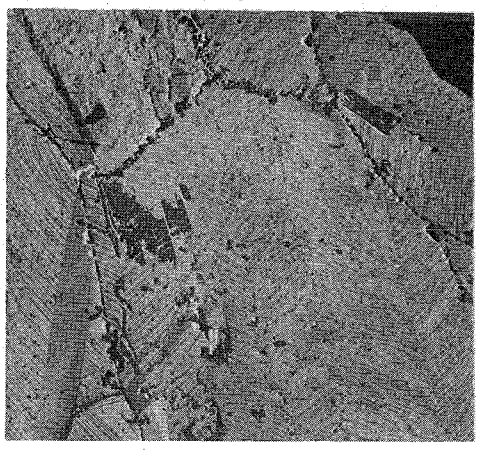

~500 μm from reaction interface

FIG. 14	INCOLOY 800 mill-annealed and then annealed for 300 hrs at 700°C in contact with UC

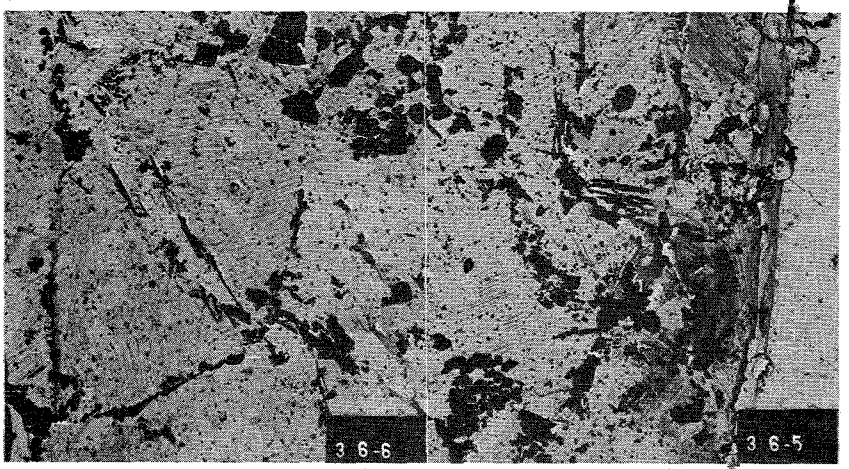

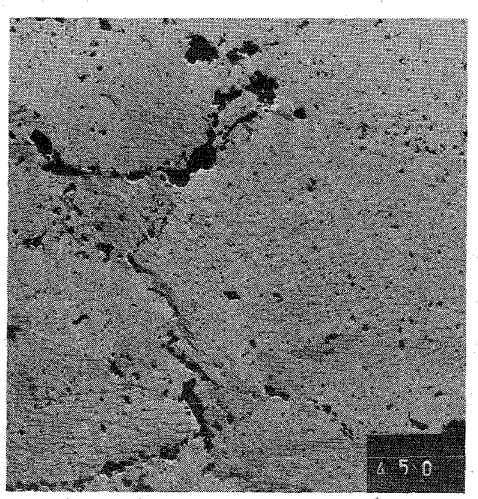

~500 µm from reaction interface

FIG. 15	INCOLOY 800 mill-annealed and then annealed for 300 hrs at 800°C in contact with UC

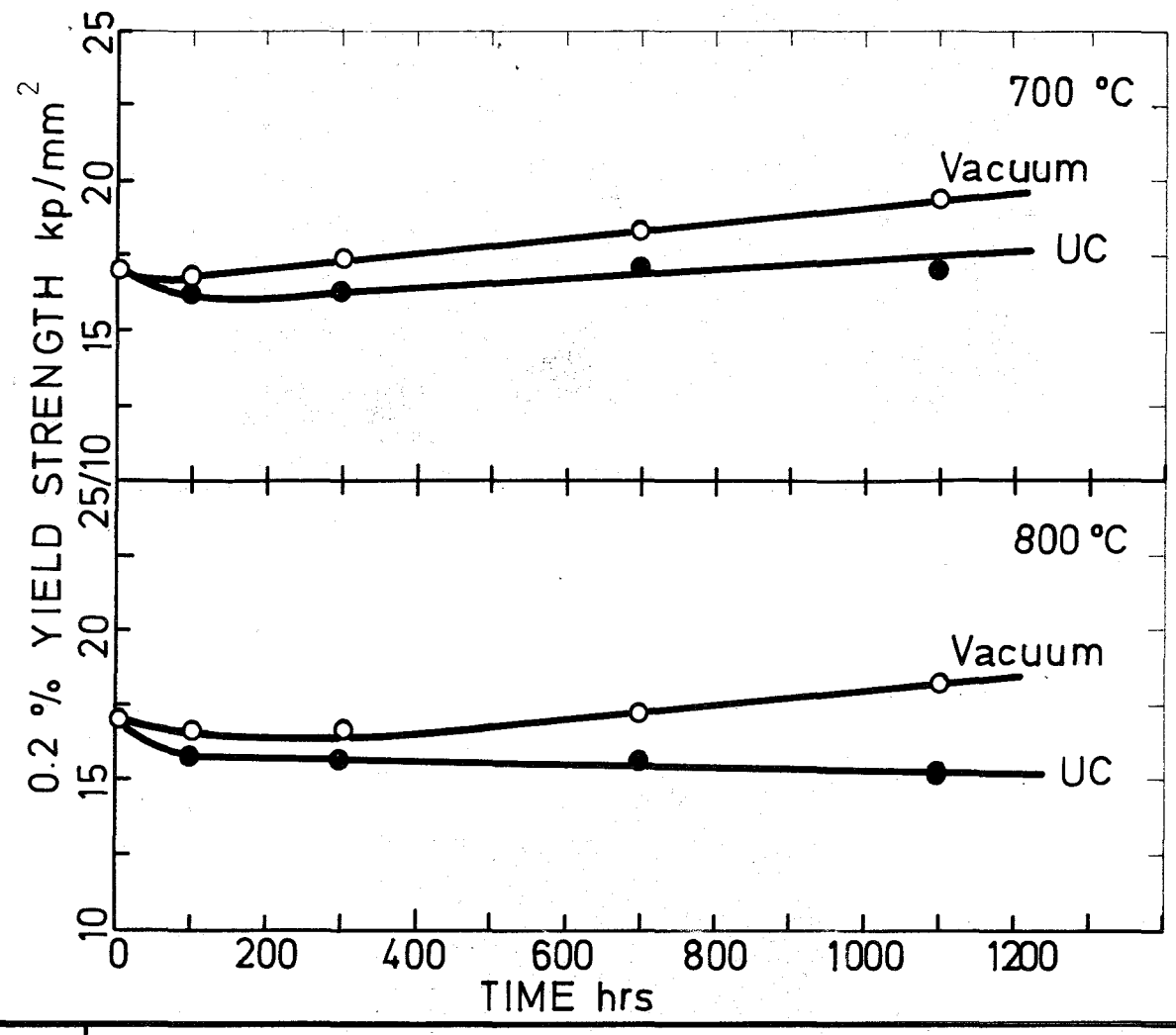

FIG. 16 Room temperature yield strength of INCOLOY 800, solution treated and then annealed in vacuum (—o—) and in contact with UC (—●—)

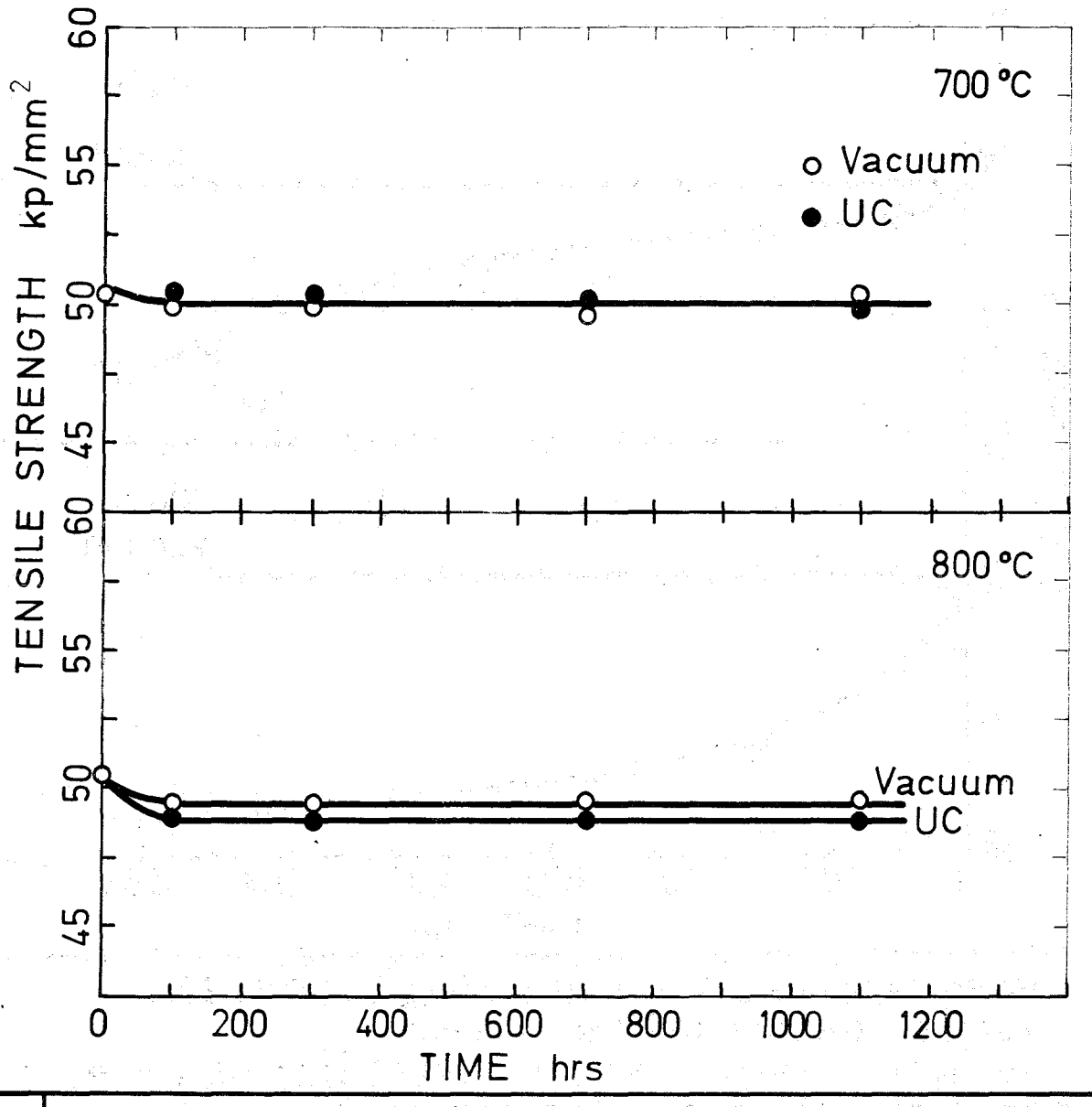

FIG. 17

Room temperature tensile strength of INCOLOY 800, solution treated and then annealed in vacuum (—o—) and in contact with UC (—●—)

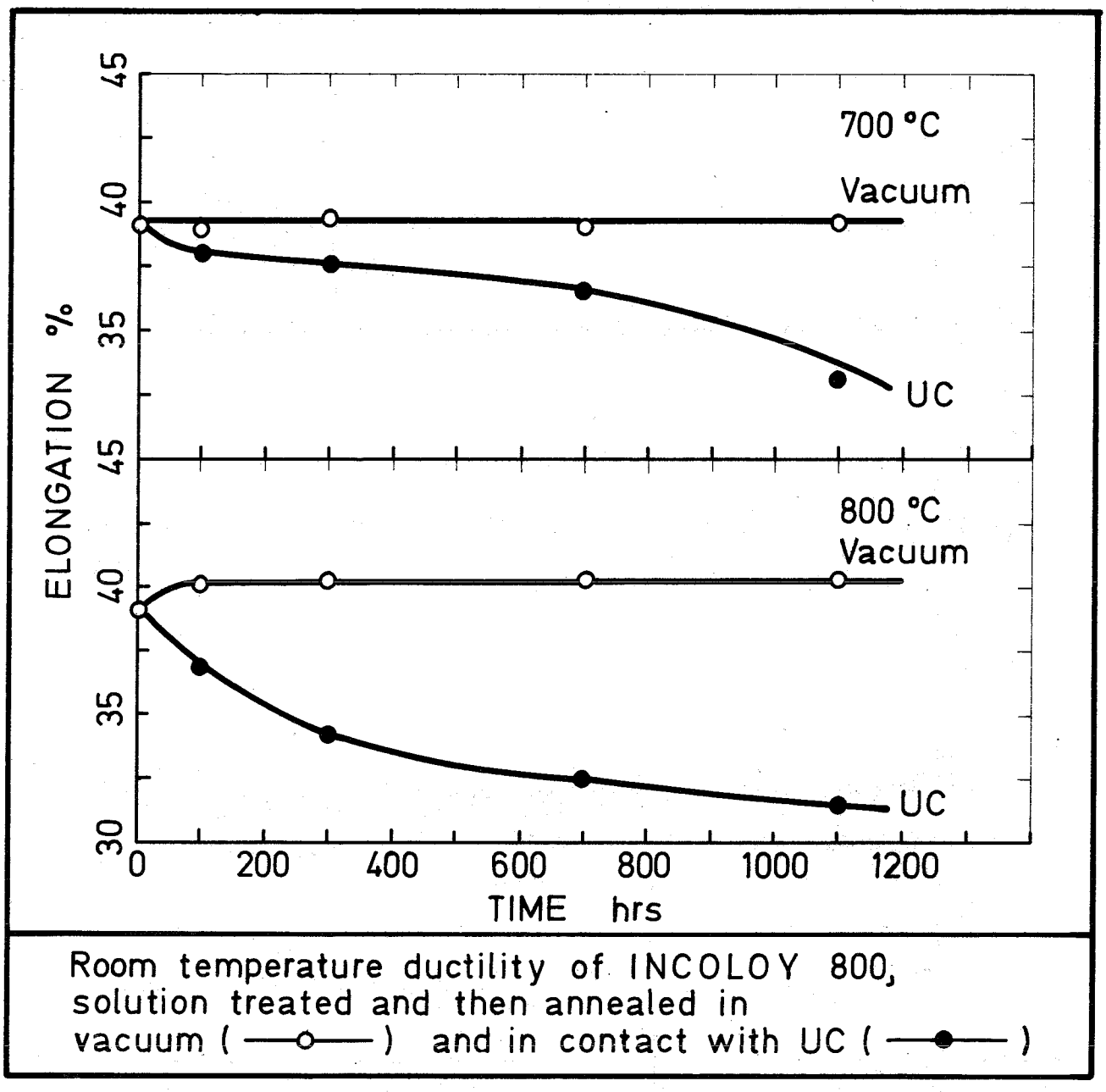

Room temperature ductility of INCOLOY 800, solution treated and then annealed in vacuum (—o—) and in contact with UC (—●—)

FIG. 18

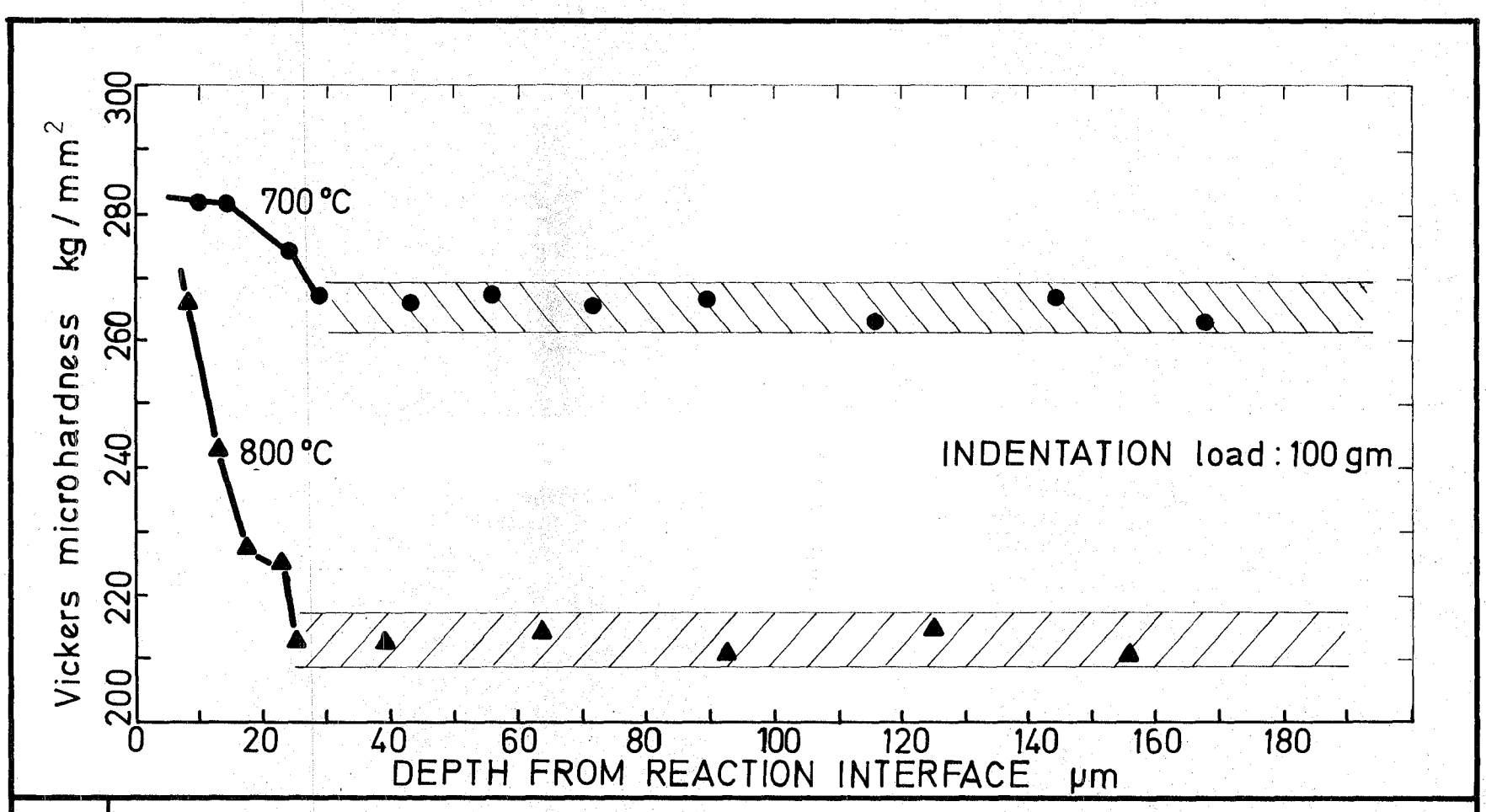

FIG. 19 Microhardness gradients in INCOLOY 800, solution treated and then annealed in contact with UC for 1100 hrs at 700 °C and 800 °C.

6 µm

near reaction interface

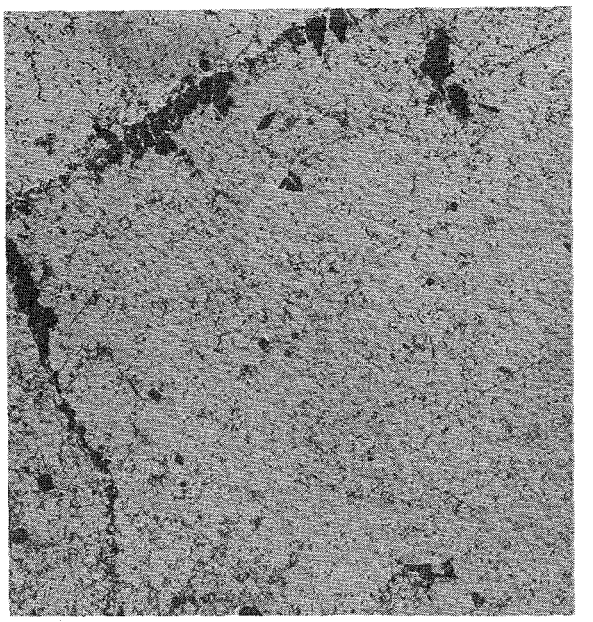

6µm

~500µm from reaction interface

300 HRS AT 700°C

6 µm

near reaction interface

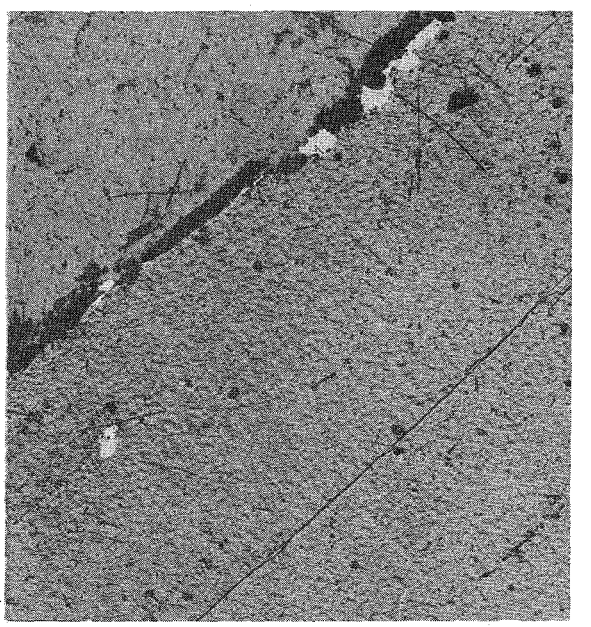

6µm

~500µm from reaction interface

300 HRS AT 800°C

FIG. 20	INCOLOY 800 solution treated and then annealed for 300 hrs at 700 and 800°C in contact with UC

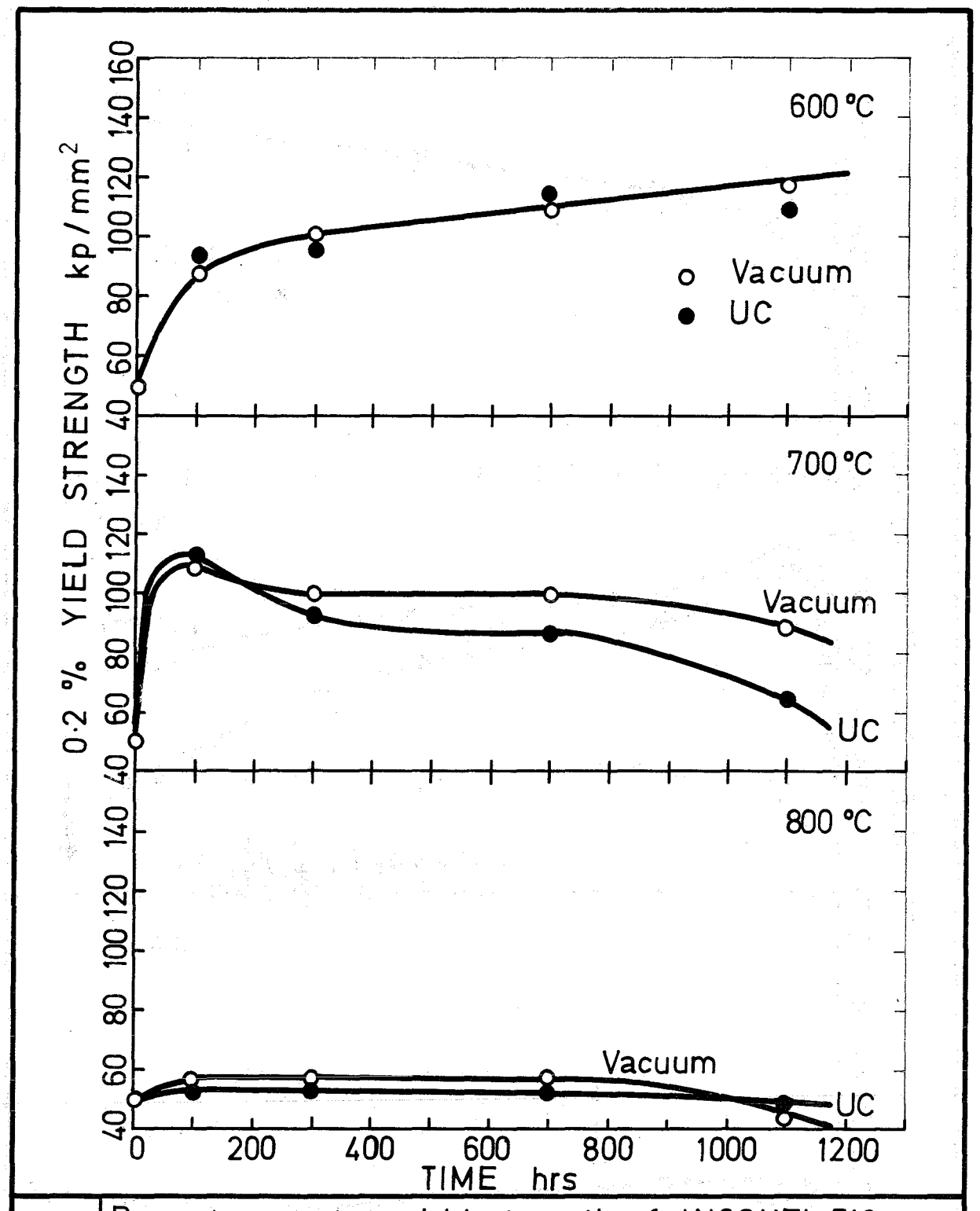

FIG. 21

Room temperature yield strength of INCONEL 718, solution treated and annealed in vacuum (—o—) and in contact with UC (—●—)

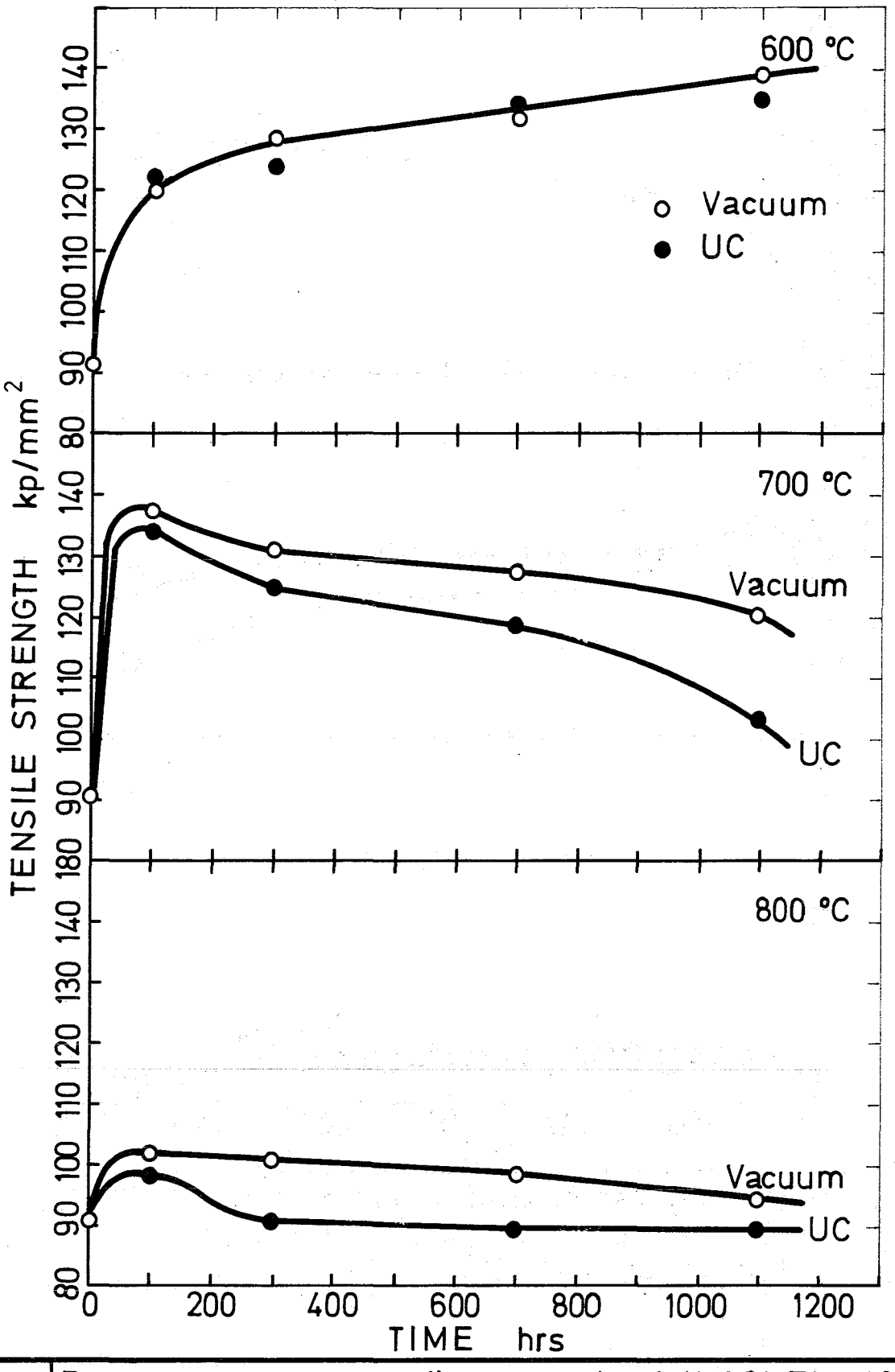

FIG. 22 Room temperature tensile strength of INCONEL 718, solution treated and annealed in vacuum (—o—) and in contact with UC (—●—)

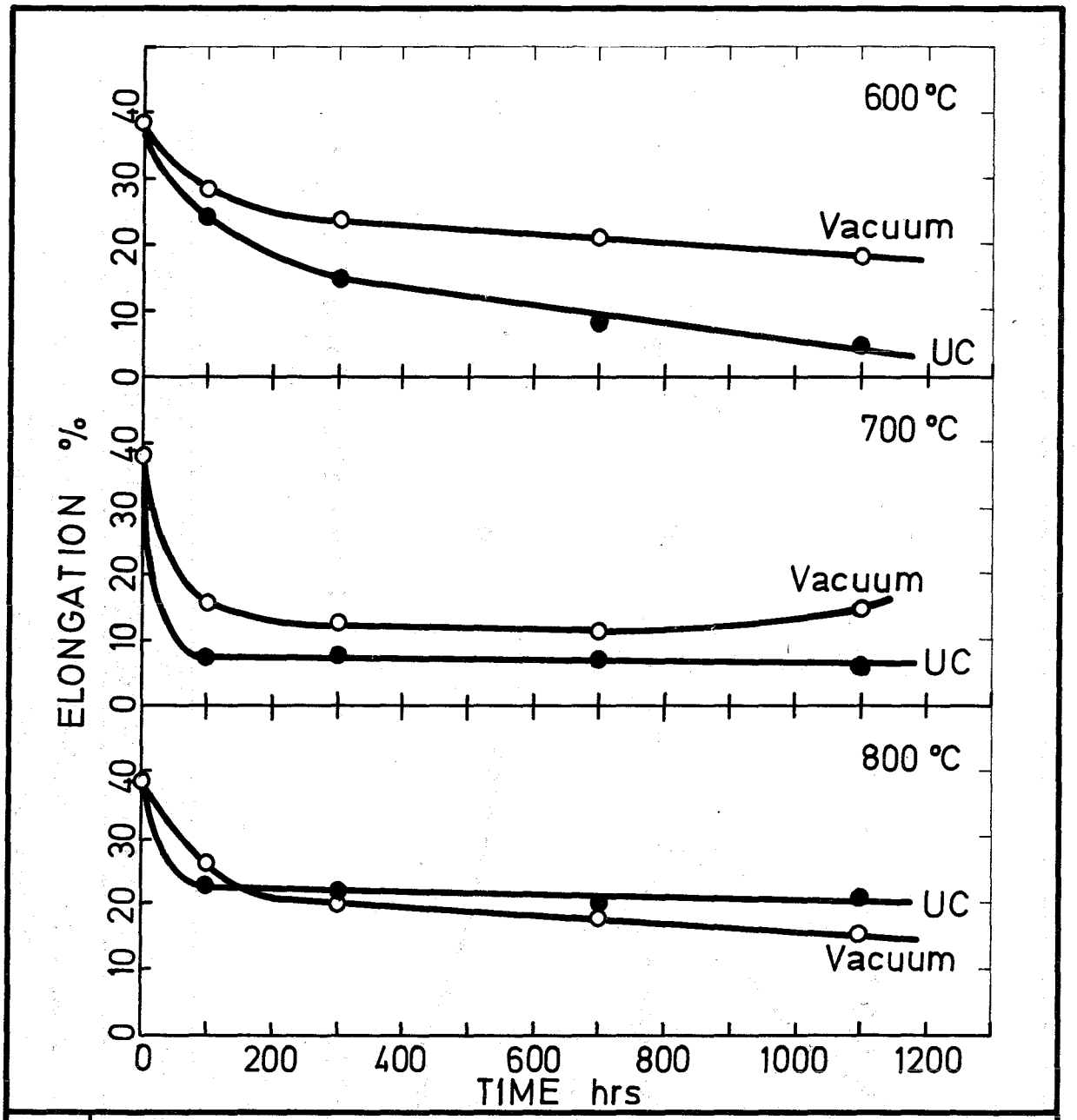

FIG. 23 Room temperature ductility of INCONEL 718, solution treated and annealed in vacuum (—o—) and in contact with UC (—●—)

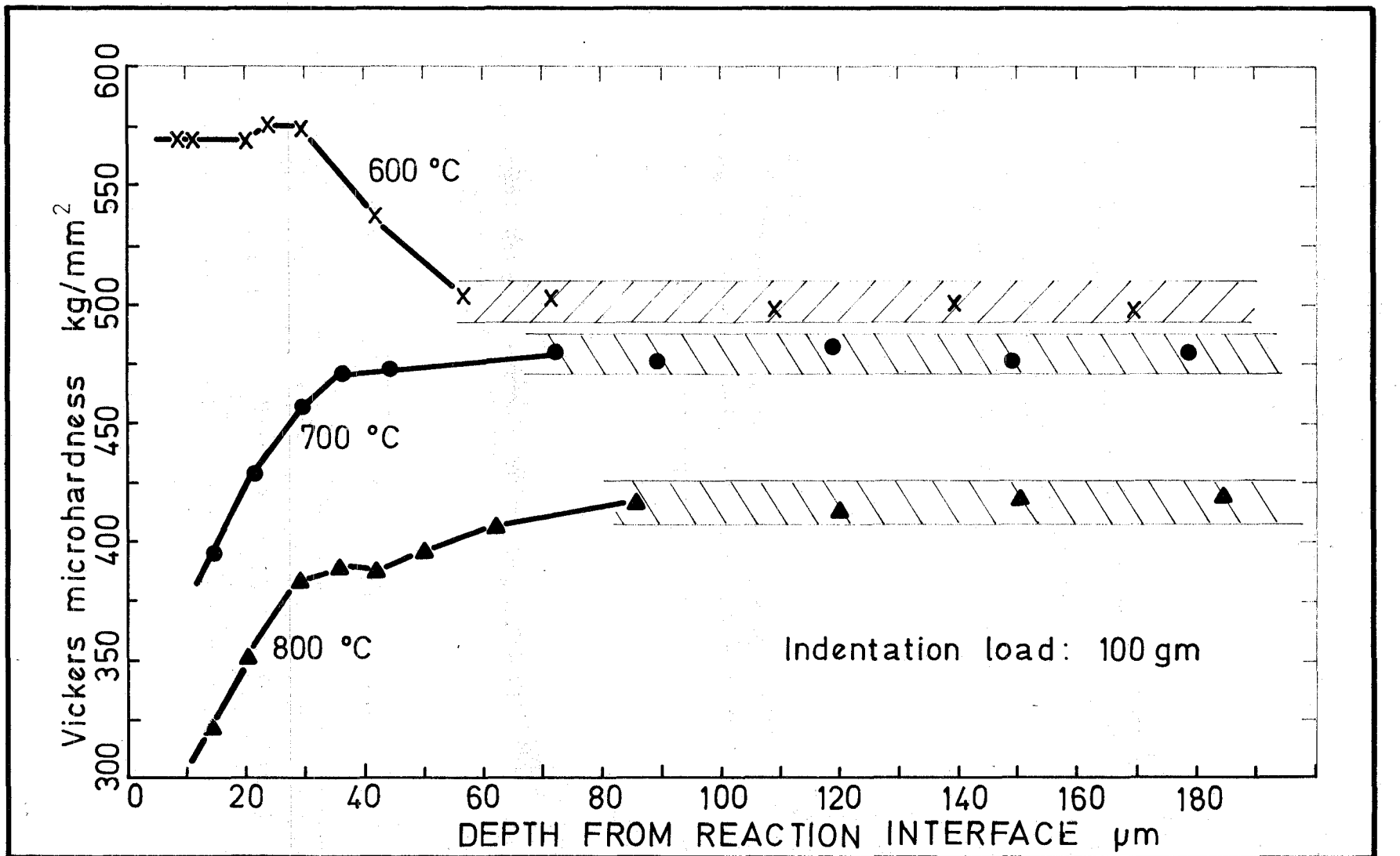

FIG. 24 Microhardness gradients in INCONEL 718, solution treated and then annealed in UC for 1100 hrs at 600, 700 and 800 °C.

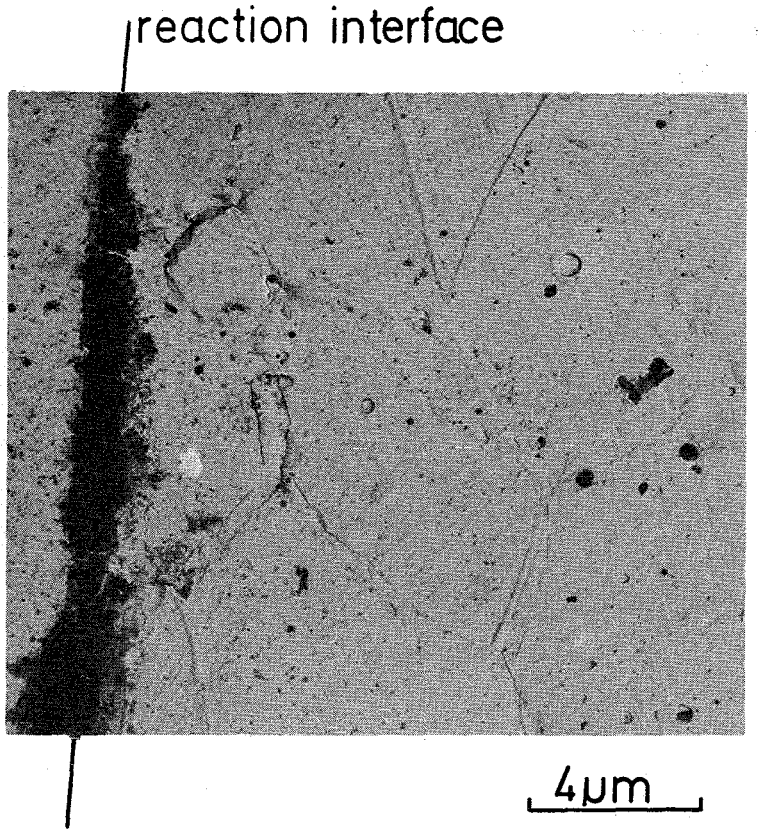

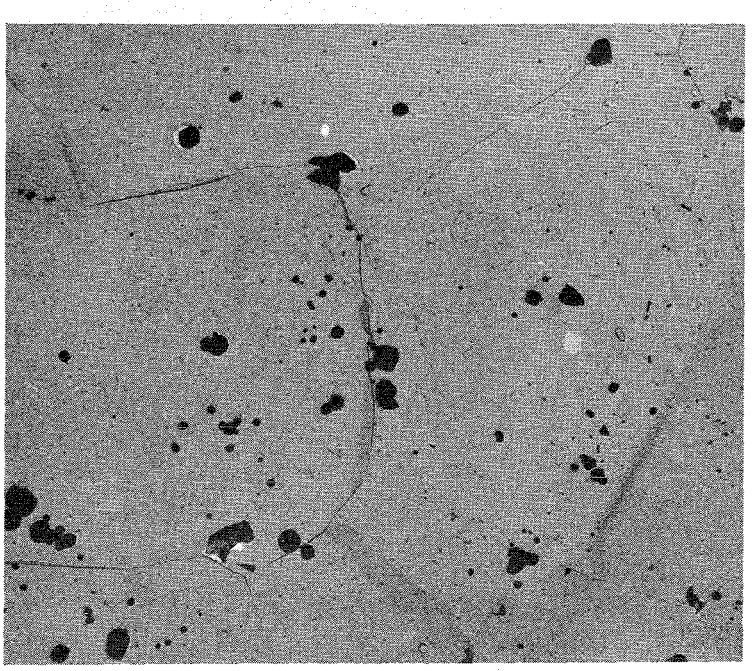

~500 μm from reaction interface

FIG. 25	INCONEL 718 solution treated and then annealed for 1100 hrs at 600°C in contact with UC

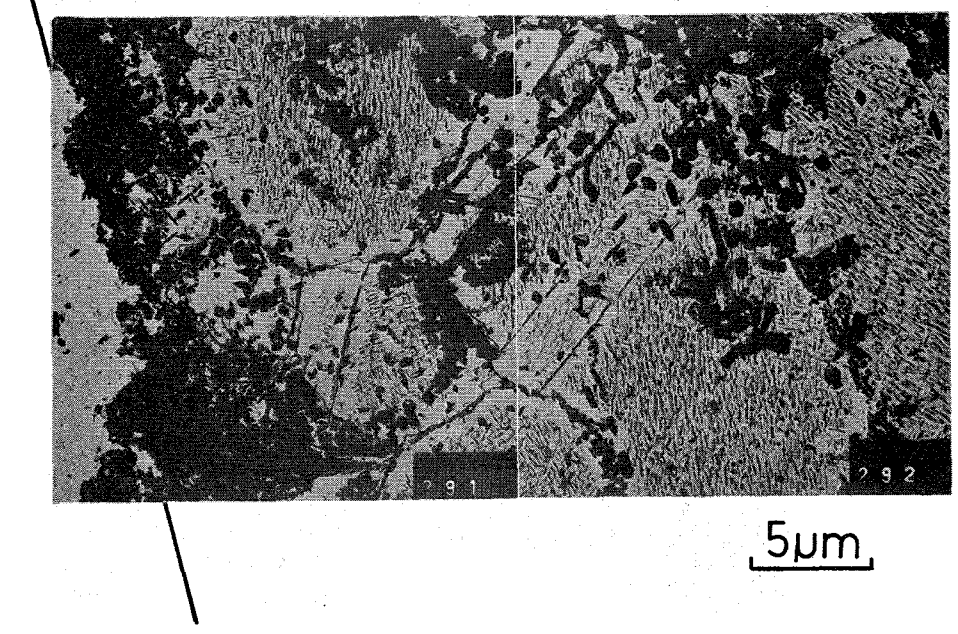

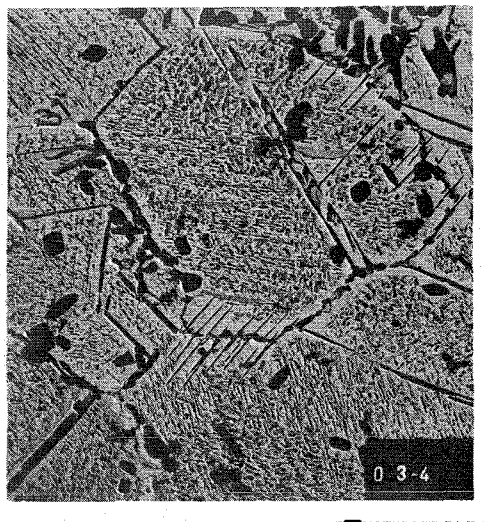

~500μm from reaction interface

FIG. 26	INCONEL 718 solution treated and then annealed for 1100 hrs at 700°C in contact with UC

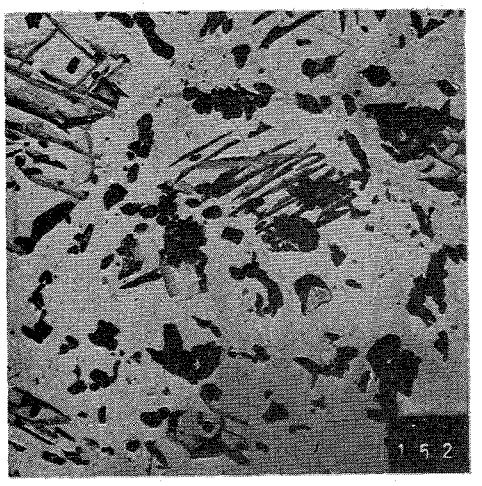

10 μm

~60μm from reaction interface

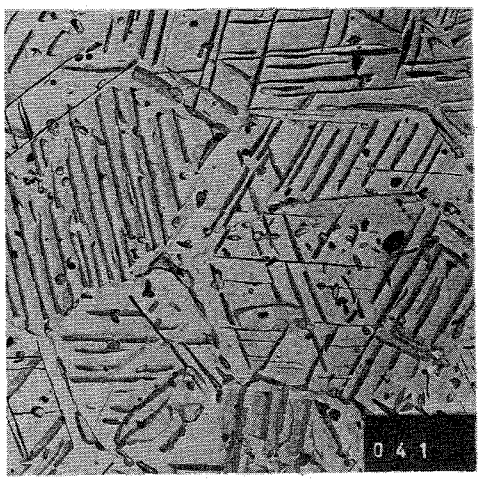

10 μm

~500 μm from reaction interface

10 μm

reaction interface

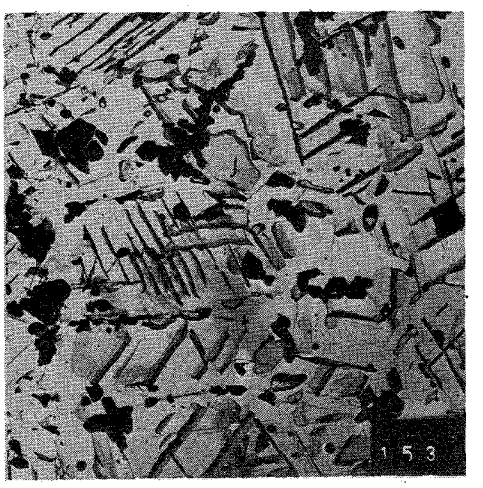

10 μm

~120 μm from reaction interface

FIG. 27

INCONEL 718 solution treated and then annealed for 1100 hrs at 800°C in contact with UC